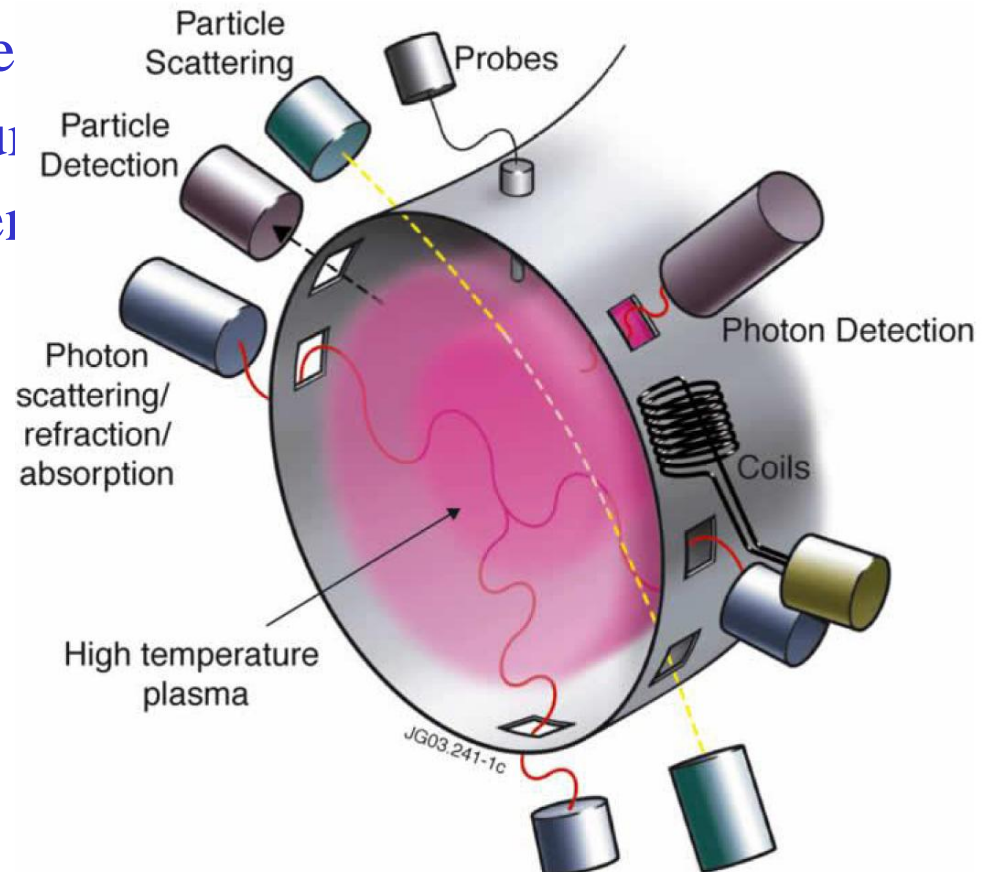


# Diagnostics

- Research topics with tokamak diagnostics
- Tokamak Diagnostics
  - Magnetic measurements
  - Electron density measurement
  - Electron temperature measurement
  - Ion temperature measurement
  - Radiation measurements
  - q-profile measurements
  - Fluctuation measurements
  - Edge probe measurements



# Research Topics with Tokamak Diagnostics

- Establishment of stable plasmas and the investigation of MHD instabilities: magnetic diagnostics, MSE, Polarimetry, soft X-ray array, Mirnov coils, etc
- Determination of energy and particle confinement times, and transport coefficients: diamagnetic loop, interferometry, reflectometry, Thomson scattering, ECE, Doppler broadening of impurity lines, neutron flux, etc
- Development of auxiliary plasma heating methods: X-ray PHA, Neutral particle analyzer, etc
- Study and control of plasma impurities: spectroscopy, Langmuir probes for edge and divertor regions, etc
- Investigation of plasma fluctuations to determine their role in plasma transport: HIBP, e.m. wave scattering, probes, etc

# ITER Diagnostic Requirements

Operating Scenario	Special Features	Required Measurements
H phase. Inductive. Ohmic L mode. Limited H Mode		Plasma shape and position, vertical speed, $B_{tor}$ , $I_p$ , $V_{loop}$ , locked modes, $m = 2$ modes, low $m/n$ MHD modes, $q(a)$ , halo current, line-averaged density, runaway electrons, impurity identification and influx, $n_e(r)$ and $T_e(r)$ in core, $T_i$ in core, surface temperature of divertor plates and first wall, $P_{rad}$ from core, line-averaged $Z_{eff}$ , H/L mode indicator, gas pressure and composition (divertor and duct)
D phase. Inductive. ELMY H mode	Exploration of H mode and initial fusion operation	As above plus: $\beta$ , $q(95\%)$ , ELM occurrence and type, $n_e(r)$ and $T_e(r)$ at edge, $P_{fus}$ , $P_{rad}(r)$ , heat deposition profile in divertor, divertor detachment,
High power D/T phase. Inductive. ELMY H Mode	Full exploration of H mode and fusion performance	As above plus: shape and position (500 s), neutron and alpha source profiles, $v_{tor}(r)$ and $v_{pol}(r)$ , impurity profile, $T_i(r)$ in core, $Z_{eff}(r)$ , $n_{He}(r)$ , $n_{He}$ in divertor, $n_T/n_D$ in core, D and T influx, divertor ionisation front position, neutral density (near wall), $n_e$ and $T_e$ in divertor, impurity and DT influxes in divertor with spatial resolution, alpha loss, neutron fluence, erosion of divertor tiles.
D/T Phase. Inductive ELMY H mode. High $\beta$	Extension to high $\beta$ including stabilisation of NTMs	As above plus: localisation of $q = 1.5$ and $q = 2$ surfaces, high sensitivity measurements of $n_e$ and $T_e$ , detection and measurement of NTMs.
Hybrid operation	Extension to long pulse using current drive	As above plus: shape and position (for 1000 s)
Steady state operation	Extension to steady state using current drive, stabilisation of NTMs and RWMs, and possibly ITBs.	As above: plus $q(r)$ (in particular location and value of $q_{min}$ ), high resolution measurements of the gradient of $T_e$ and $T_i$ , measurement of RWMs.

# ITER Diagnostics I

Selected Diagnostic System	Parameters Measured
<b>Magnetic Diagnostics</b>	
<p>Coils and loops mounted on the interior surface of the vacuum vessel. Halo current sensors mounted on the blanket shield module supports. <i>Coils mounted between the vacuum vessel skins.</i> Rogowski coils and <i>loops</i> mounted on the exterior surface of the vacuum vessel. Coils mounted in the divertor.</p>	<p>Plasma Current, Plasma Position and Shape, Loop Voltage, Plasma Energy, Locked-modes Low (m,n) MHD Modes, Sawteeth, Disruption Precursors, Halo Currents, Toroidal Magnetic Field, Static error field of PF and TF, High Frequency macro instabilities (Fishbones, TAE Modes)</p>
<b>Fusion Product Diagnostics</b>	
<p>Radial Neutron Camera, <i>Vertical Neutron Camera</i>, Micro-fission Chambers (N/C) Neutron Flux Monitors (Ex-Vessel) Gamma-Ray Spectrometer Activation System, <i>Lost Alpha Detectors (N/C)</i> <i>Knock-on Tail Neutron Spectrometer (N/C)</i></p>	<p>Total Neutron source strength, <i>Neutron/Alpha source profile</i>, Fusion Power, Fusion power density, Ion temperature profile, Neutron fluence on the first wall, nT/nD in plasma core, <i>Confined alpha particles</i>, <i>Energy and Density of escaping alphas</i></p>
<b>Optical/IR(Infra-Red) Systems</b>	
<p>Core Thomson Scattering Edge Thomson Scattering , X-Point Thomson Scattering, <i>Divertor Thomson Scattering</i> Toroidal Interferometer/ Polarimeter, <i>Polarimeter (Poloidal Field Measurement)</i> <i>Collective Scattering System</i></p>	<p>Line-Averaged Electron Density Electron Temperature Profile (Core and Edge) Electron Density Profile (Core and Edge) <i>Current profile</i> <i>Divertor Electron Parameters</i> <i>Confined alpha particles.</i></p>
<b>Bolometric Systems</b>	
<p>Bolometer arrays mounted in the ports, in the divertor and <i>in the vacuum vessel.</i></p>	<p>Total Radiated power, Divertor radiated power <i>Radiation profile (core and divertor)</i></p>

# ITER Diagnostics II

<b>Spectroscopic and Neutral Particle Analyser Systems</b>	
H Alpha Spectroscopy, Visible Continuum Array Main Plasma and <i>Divertor Impurity Monitors</i> , X-Ray Crystal Spectrometers, Charge eXchange Recombination Spectroscopy (CXRS) based on DNB, <i>Motional Stark Effect (MSE) based on heating beam</i> , <i>Soft X-Ray Array (N/C)</i> , Neutral Particle Analysers (NPA), <i>Laser Induced Fluorescence (N/C)</i>	Ion temperature profile, Core He density, Impurity density profile, Plasma rotation, ELMs, L/H mode indicator, nT/nD & nH/nD in the core, edge and divertor, Impurity species identification, Impurity influx, <i>Divertor He density</i> , Ionisation front position, Zeff profile, Line averaged electron density, <i>Confined alphas</i> , <i>Current density profile</i> .
<b>Microwave Diagnostics</b>	
Electron Cyclotron Emission (ECE) Main Plasma Reflectometer Plasma Position Reflectometer, Divertor Interferometer/ <i>Reflectometer</i> , <i>Divertor EC absorption (ECA)</i> , Main Plasma Microwave Scattering, <i>Fast Wave Reflectometry (N/C)</i>	Plasma position and shape, Locked Modes Low (m,n) MHD Modes, Sawteeth, Disruption Precursors, Plasma Rotation, H-mode indicator Runaway electrons, Electron Temperature Profile, Electron Density Profile, High Frequency micro-instabilities, <i>Divertor electron parameters</i> .
<b>Plasma-Facing Components and Operational Diagnostics</b>	
IR/Visible Cameras, Thermocouples, Pressure Gauges, Residual Gas Analysers, <i>IR Thermography (Divertor)</i> , <i>Langmuir Probes</i>	Runaway electrons: energy and current Gas pressure and composition in divertor Image and temperature of first wall Gas pressure and composition in main chamber and duct, <i>Escaping alphas</i> , Ion flux, ne and Te at divertor plates, <i>Surface temperature and power load in divertor</i> .

*Systems with implementation difficulties, and the physical parameters that currently have an uncertain measurement capability, are shown in italics. N/C: new concept technique.*

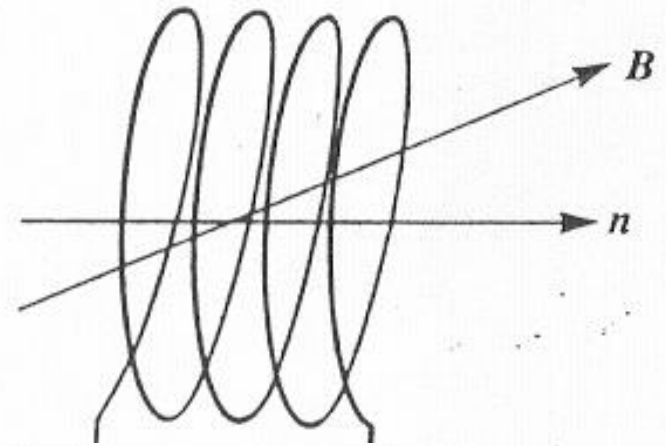
# Diagnostics for Real-Time Feedback Control at JT-60U

Quantity	Objectives	Applications
<ul style="list-style-type: none"> <li>• Averaged electron density (FIR/ CO<sub>2</sub> interferometer, CO<sub>2</sub> Polarimeter)</li> <li>• Neutron emission rate (fission chamber)</li> <li>• Plasma stored energy (diamagnetic loop)</li> <li>• Central electron temp. (ECE measurement)</li> <li>• Electron Temperature gradient (ECE measurement)</li> <li>• Electron Temperature fluctuations (ECE measurement)</li> <li>• Ion Temperature profile (CXRS measurement)</li> <li>• Current density profile (MSE polarimeter)</li> <li>• Main plasma radiation (bolometers)</li> </ul>	<ul style="list-style-type: none"> <li>• Optimize target and operation density</li> <li>• Control stability, fusion burn</li> <li>• Control stability, avoid disruption</li> <li>• Optimize target temperature</li> <li>• Control internal transport barrier</li> <li>• Suppress neoclassical tearing mode</li> <li>• Control internal transport barrier (Optimize target temperature)</li> <li>• Control q profile</li> <li>• Improve confinement by enhanced radiation</li> </ul>	<ul style="list-style-type: none"> <li>• Versatile in a variety of exp.</li> <li>• Establish route toward high QDT* in R/S plasmas</li> <li>• Sustain plasma performance in a steady-state</li> <li>• Study non-inductive CD, High Te / Ti confinement</li> <li>• Sustain bootstrap current for a steady-state operation</li> <li>• Sustain high performance in a steady-state</li> <li>• Sustain AT modes</li> <li>• Sustain AT modes</li> <li>• Optimize radiation mantle</li> </ul>
<ul style="list-style-type: none"> <li>• Outer gap distance (magnetics &amp; equilibrium)</li> </ul>	<ul style="list-style-type: none"> <li>• Keep stable RF coupling, investigate wall effect on stability</li> </ul>	<ul style="list-style-type: none"> <li>• Sustain R/S plasmas by LHRF, improve stability in R/S plasmas</li> </ul>
<ul style="list-style-type: none"> <li>• Divertor electron density (mm-wave interferometer)</li> <li>• Divertor pressure (ionization gauge)</li> <li>• Divertor radiation (bolometers)</li> </ul>	<ul style="list-style-type: none"> <li>• Optimize divertor density</li> <li>• Control MARFE/detachment</li> <li>• Reduce divertor heat load</li> </ul>	<ul style="list-style-type: none"> <li>• Control divertor plasma</li> <li>• Sustain radiative divertor</li> <li>• Explore radiative divertor</li> </ul>

# Magnetic Measurements

$$\Phi = -\int_{t_0}^t V(t') dt' = NAB\vec{B} \cdot \vec{n}$$

Measure magnetic field, flux, loop voltage, current, and plasma energy

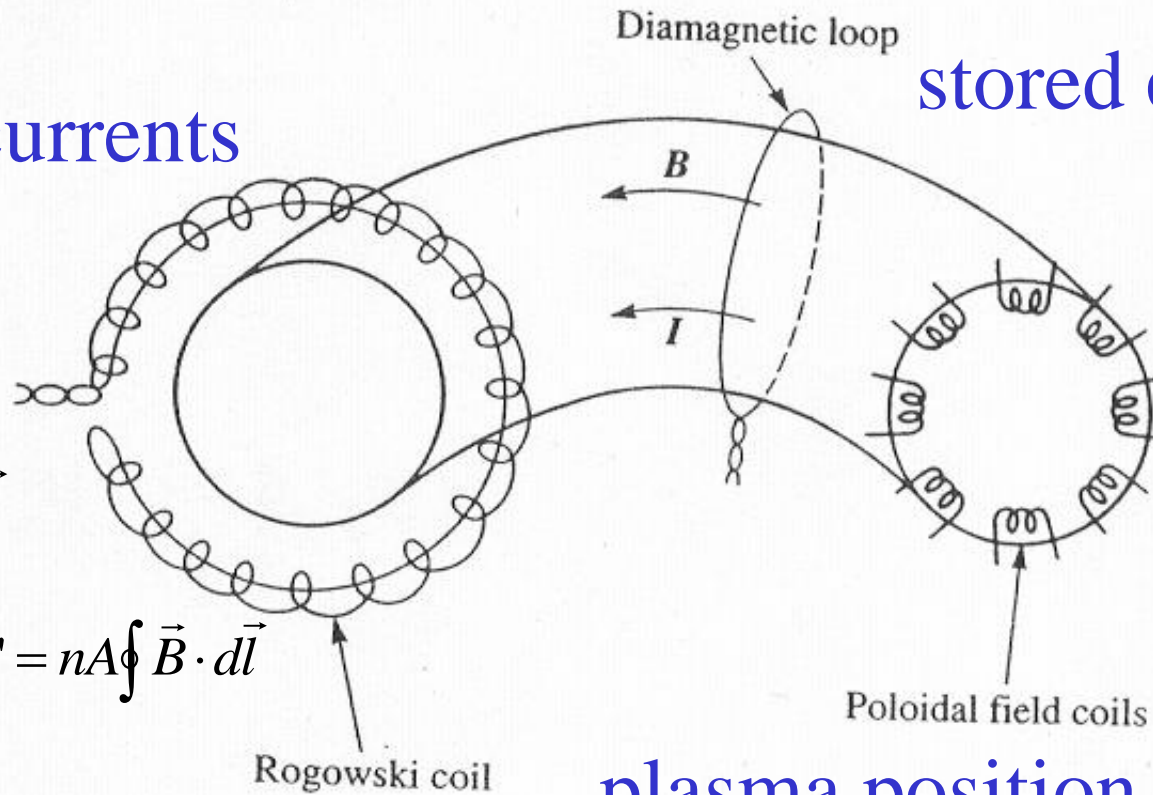


plasma currents

stored energy

$$I = \frac{1}{\mu_0} \oint \vec{B} \cdot d\vec{l}$$

$$\Phi = -\int_{t_0}^t V(t') dt' = nA \oint \vec{B} \cdot d\vec{l}$$



plasma position and shape

# Loop Voltage and Plasma Surface

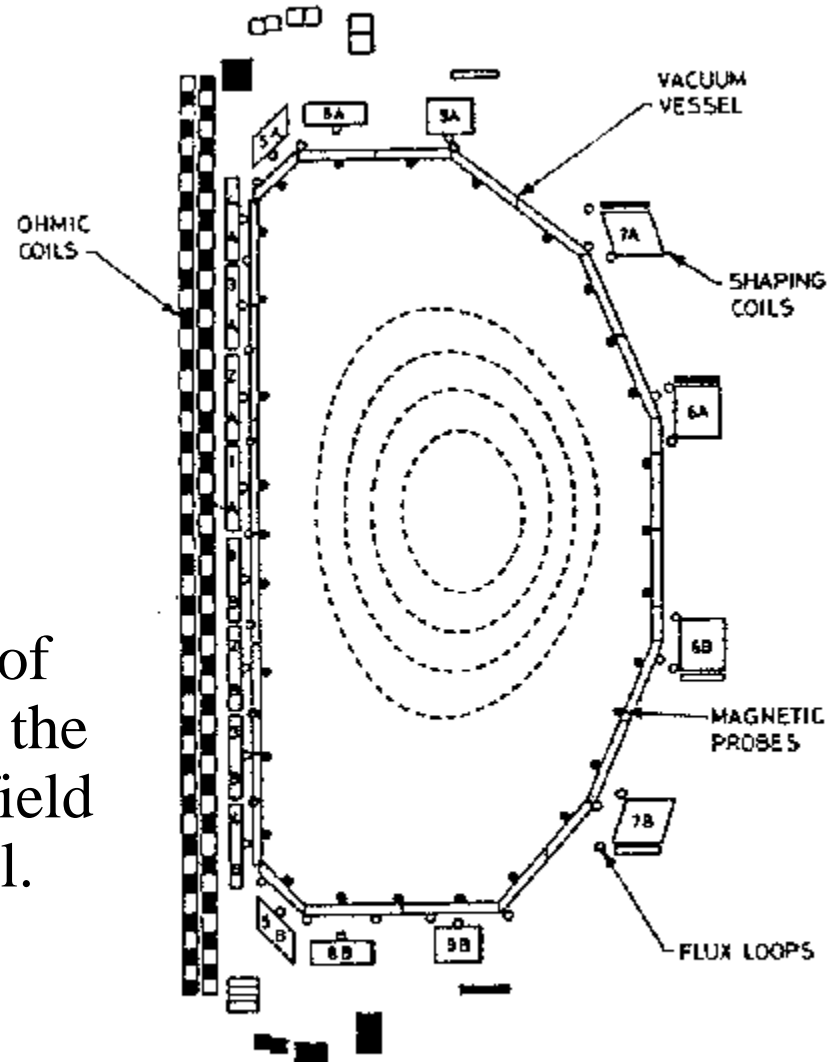
**Loop voltage:**  $V_{loop} = I_p R_p$   
voltage induced by flux changes  
due both to the primary circuit  
and the plasma current itself

## Plasma surface:

The shape and position of the  
outermost closed magnetic surface of  
the plasma can be determined from the  
toroidal loop voltage and poloidal field  
measured around the vacuum vessel.

$$\psi \quad B_R = -\frac{1}{R} \frac{d\psi}{dZ} \quad B_Z = \frac{1}{R} \frac{d\psi}{dR}$$

extrapolate across a current-free region . *Configurations of OH, shaping and magnetic diagnostic coils in DIII-D.*





# Plasma Energy and Internal Inductance

**Diamagnetic flux:** difference between the total toroidal flux and that in the absence of plasma

from equilibrium equation, 
$$\frac{(\nabla \times \vec{B}) \times \vec{B}}{\mu_o} = \nabla p$$

cyindrical limit 
$$\frac{dp}{dr} + \frac{d}{dr} \left( \frac{B_\phi^2}{2\mu_o} \right) + \frac{B_\theta}{\mu_o r} \frac{d}{dr} (rB_\theta) = \frac{dp}{dr} + \frac{d}{dr} \left( \frac{B_\phi^2 + B_\theta^2}{2\mu_o} \right) + \frac{B_\theta^2}{\mu_o r} = 0$$

integrating over the plasma volume,

$$2\beta_{p\perp} + \beta_{p\parallel} + l_i - \mu = 2(S_1 + S_2)$$

$$\beta_{p\parallel} + l_i + \mu = 2S_2 R_T / R_o$$

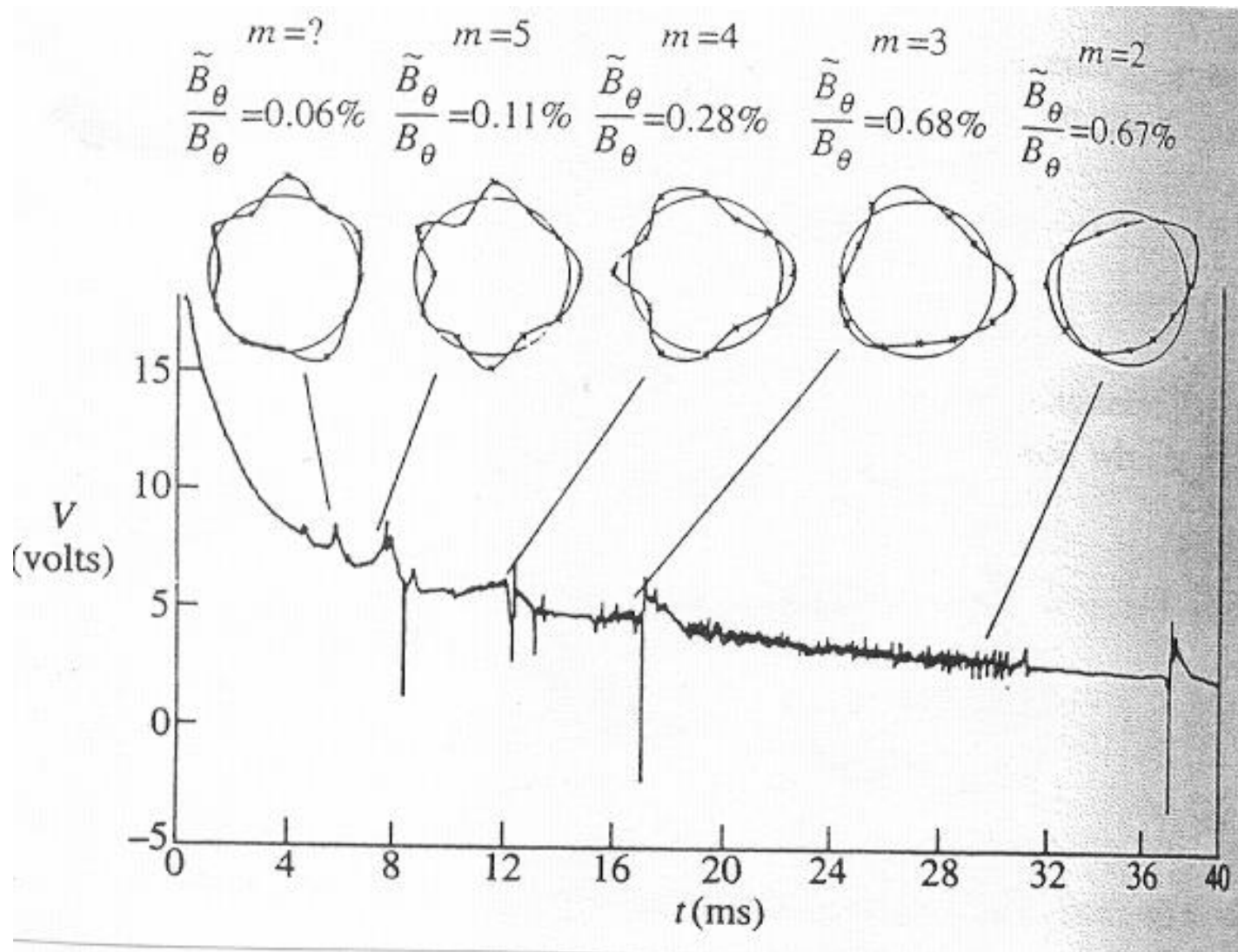
diamagnetic parameter  $\mu = \frac{8\pi B_o \Delta\phi}{\mu_o^2 I^2}$  Shafranov integrals

$$B_a^2 = \frac{\mu_o^2 I^2}{4\pi A} = \frac{\mu_o^2 I^2}{l^2} \quad \beta_p = \frac{8}{3} \frac{W}{\mu_o R_o I^2} \quad S_1 = \frac{\int B_p^2 \vec{r} \cdot d\vec{S}}{\mu_o^2 I^2 R_o} \quad S_2 = \frac{\int B_p^2 \vec{R} \cdot d\vec{S}}{\mu_o^2 I^2 R_o}$$

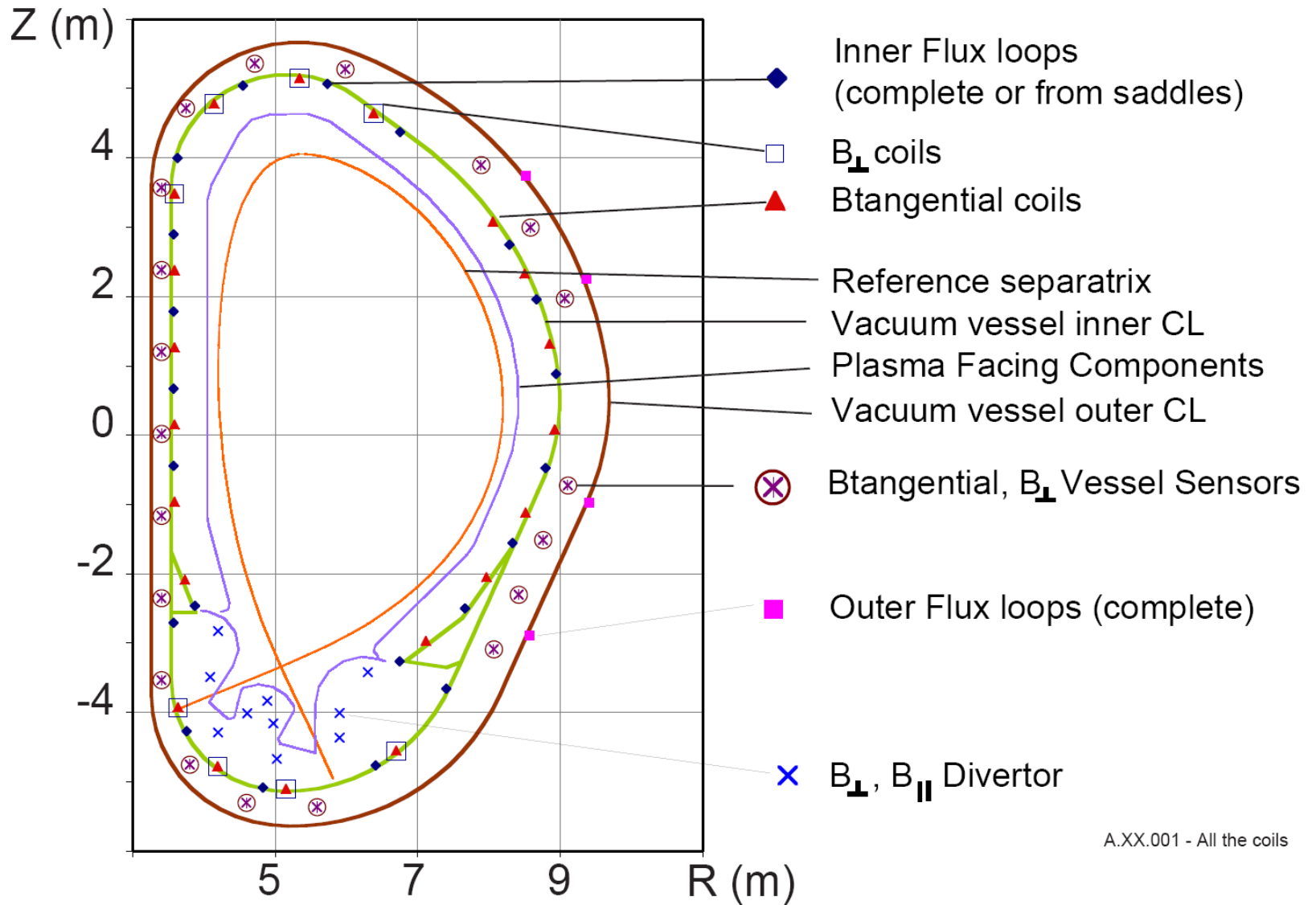
$$\beta_{p\perp} = S_1 + S_2 \left(1 - \frac{R_T}{R_o}\right) + \mu \approx 1 + \mu \quad (\beta_{p\parallel} + \beta_{p\perp}) + l_i = S_1 + S_2 \left(1 + \frac{R_T}{R_o}\right)$$

$$= \beta_{diam} \quad = 2\beta_{mhd} + l_i$$

# MHD Instability Measurements



# ITER Magnetic Diagnostics

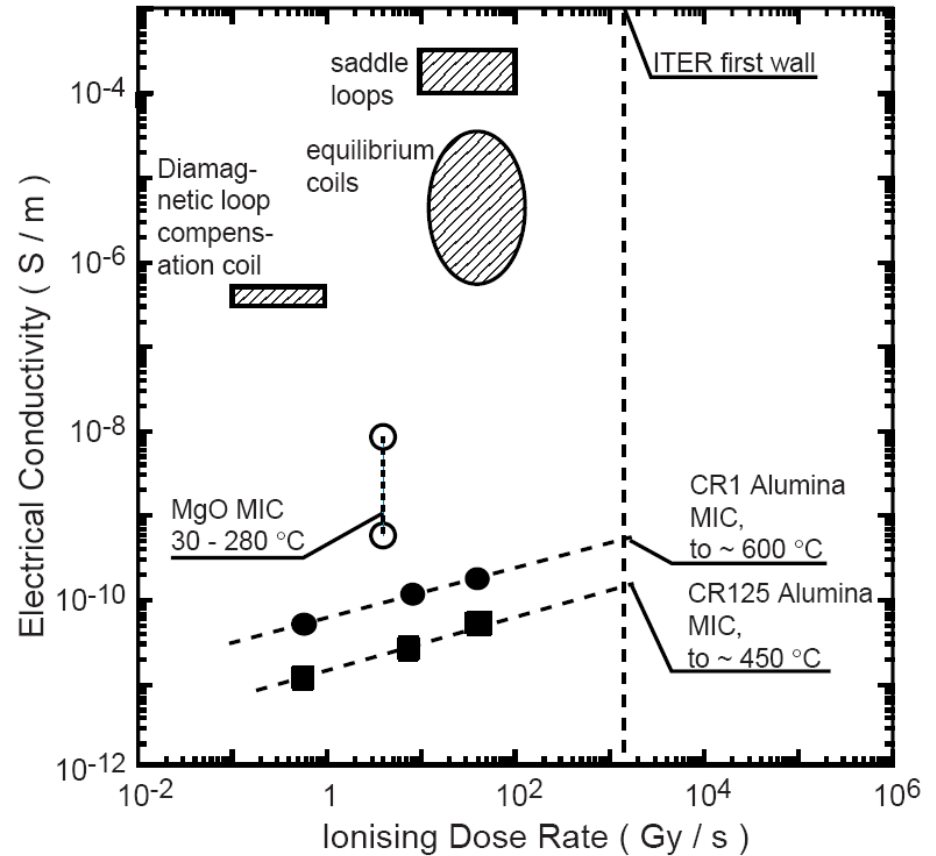
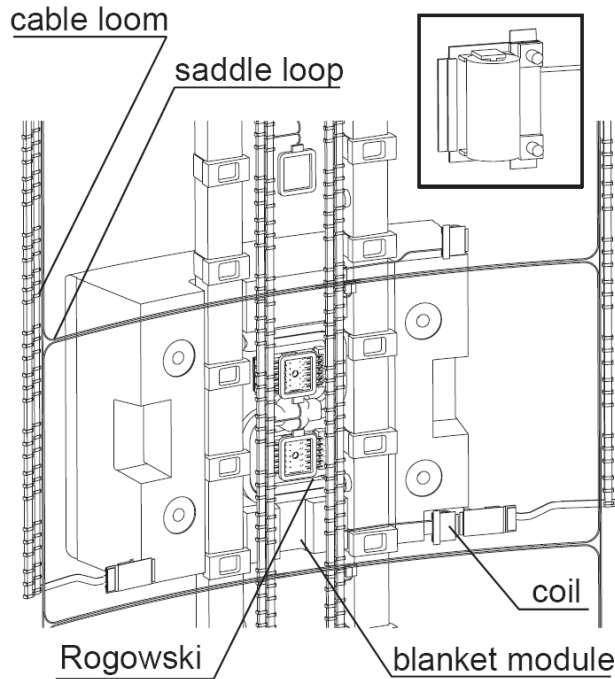


A.XX.001 - All the coils

Fig. 1. Poloidal distribution of magnetic sensors. The diamagnetic loops and external Rogowski coils are not shown.

# ITER Magnetic Diagnostics

The step to ITER requires that proper account is taken in the design for (i) nuclear heating, (ii) long pulse operation, and (iii) radiation



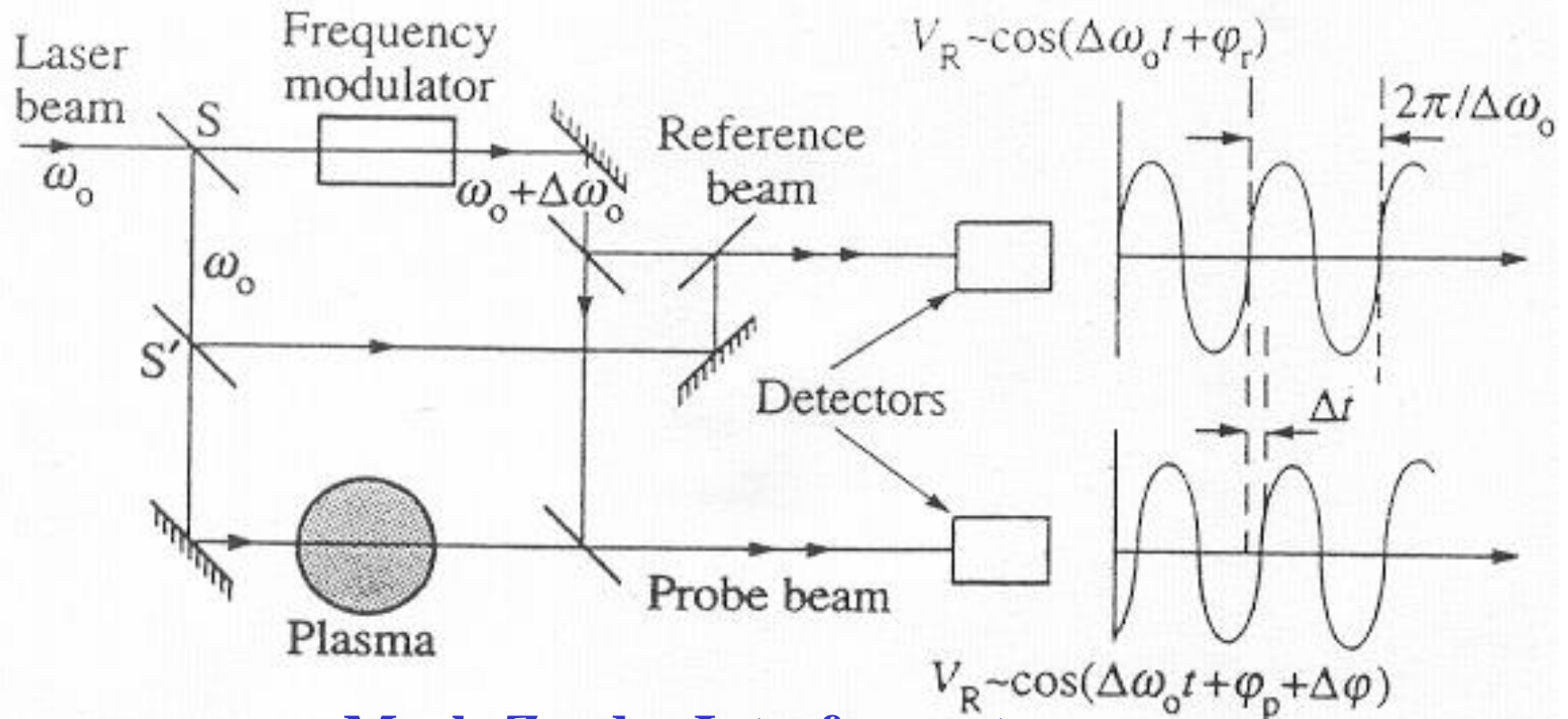
There are two radiation effects that can influence the signals – Radiation Induced Conductivity (RIC) and Radiation Induced EMF (RIEMF). A third radiation effect – Radiation Induced Electrical Degradation →

minimise this: (i) increasing the ratio of effective sensor area to cable length, (ii) reducing the temperature and radiation field asymmetries by adopting an even layer coil structure and choosing areas of expected uniform radiation level, (iii) lowering the coil resistance and hence reducing the differential voltage, and (iv) reducing the integrator sensitivity to common mode voltage by lowering the balanced impedance to ground at the input. Most of these measures

# Electron Density Measurement: Interferometry

Refractive index  $\mu = 1 - \omega_p^2 / \omega^2$

Phase change due to plasma density  $\Delta\phi = \frac{\lambda e^2}{4\pi\epsilon_0 m_e c^2} \int n_e dl$



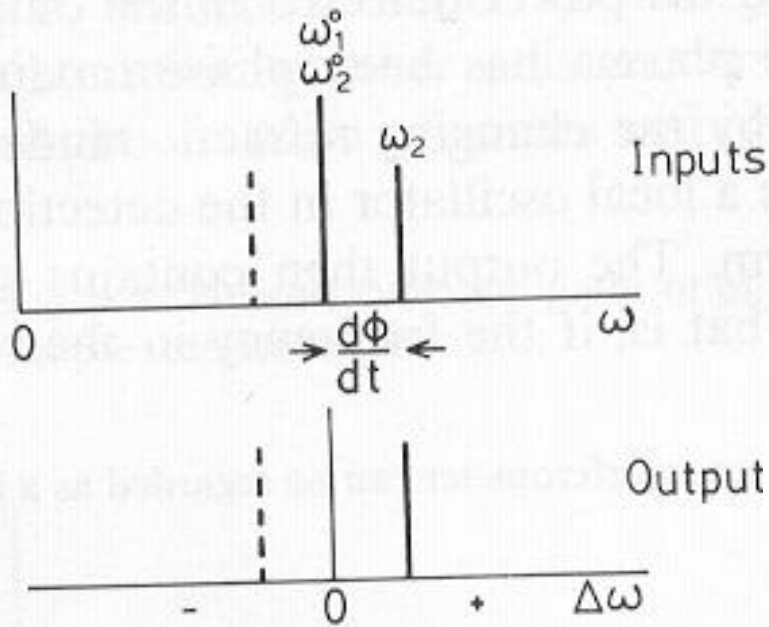
**Mach-Zender Interferometer**

# Design of Interferometry

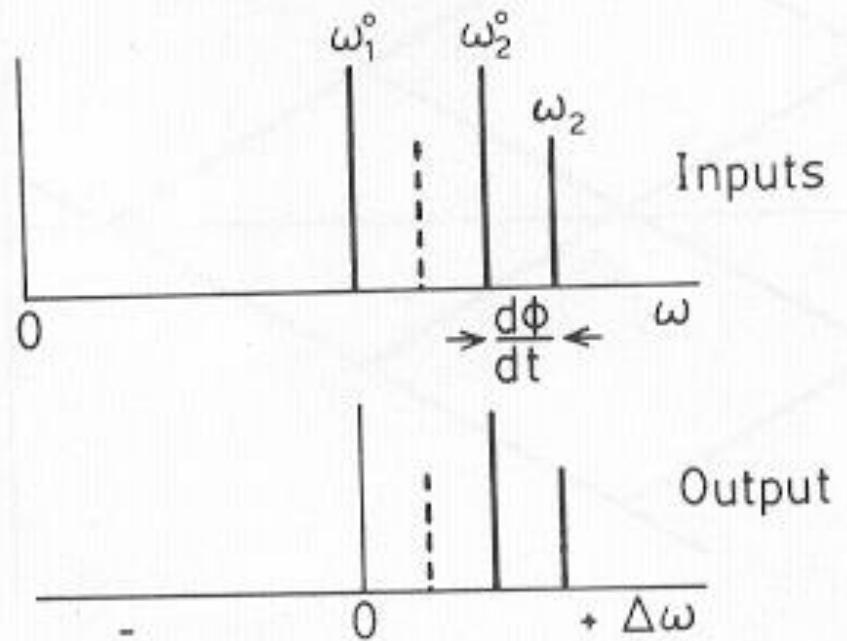
- Types of interferometers
  - Michelson, Mach-Zender, Fabry-Perot interferometers
  - homodyne and heterodyne
- Frequency sources
  - sensitive to the electron density:  $\Delta\phi \propto \lambda \int n_e dl$
  - insensitive to mechanical vibrations: long wavelength
  - small refraction of the beams: short wavelength
  - wavelengths between 10 and 2000  $\mu m$  are used
- Beam detectors
  - room temperature pyroelectric detector: simple, inexpensive
  - liquid helium-cooled indium antimonide crystals: high sensitivity
  - Schottky diodes: good response at high frequencies
- Phase counters
  - multi-fringe, high phase resolution counter
- Inversion of line-integrated density profiles
  - Abel inversion
  - inversion using iso-density flux contours

# Types of Interferometers

## HOMODYNE



## HETERODYNE



# Relevant Parameters for Various Sources

**Table 1.** Summary of relevant parameters for various wavelengths for a tangential ( $\theta_i = 0.77$ ) double pass beam in ITER. The density resolutions assume  $\Delta\phi$  resolution of 1/100 radian and polarization resolution of 1/1000 radian.

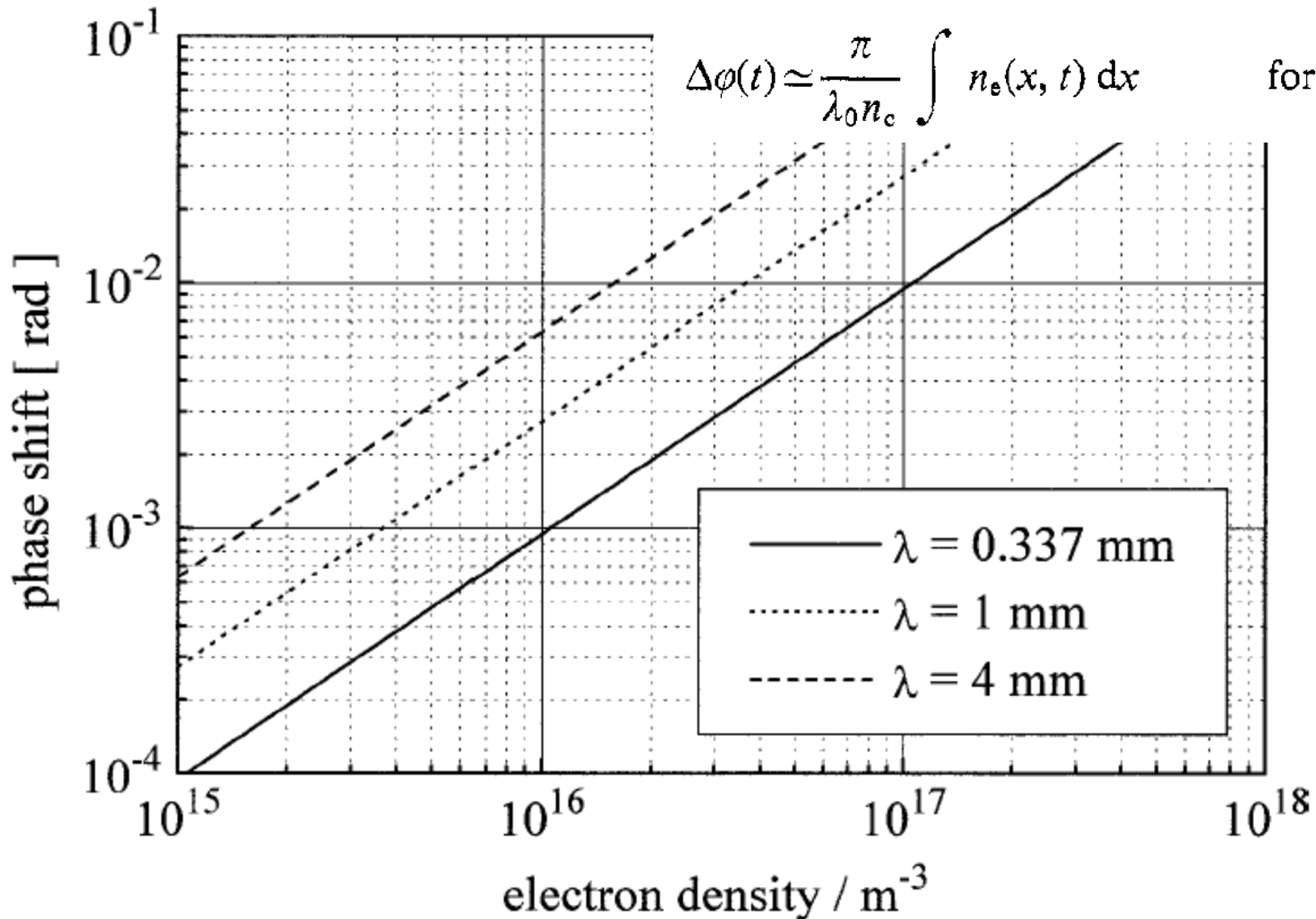
$\lambda$ ( $\mu\text{m}$ )	Port Penetration Size (cm) Retroreflector/Mirror	$\theta_i$ $n_e$ (o) ( $\times 10^{19} \text{ m}^{-3}$ )	Total Phase Shift (rad)	Faraday Rotation (rad)	Interferometer $\Delta \bar{n}_e / \bar{n}_e$ ( $\times 10^{-2}$ )	Faraday Rotation $\Delta n_e B / \bar{n}_e B$ ( $\times 10^{-2}$ )
195	74/91	13	1969	73	0.0005	0.0014
		1	151	5.6	0.006	1.8
119	44/57	13	1202	27	0.008	0.0037
		1	92	2.1	0.01	0.048
50	22/30	13	505	4.8	0.002	0.02
		1	39	0.37	0.026	0.027
10.6	10/13	13	107	0.21	0.0093	0.48
		1	8	0.016	0.12	6.2
3.39	6/8	13	34	0.022	0.029	4.5
		1	2.6	0.017	0.38	60
1	3/4	13	10	0.0019	0.1	52
		1	0.78	0.0005	1.3	666



# Sensitivity for Various Frequency Sources

$$\Delta\phi(t) = \frac{2\pi}{\lambda_0} \int \left[ 1 - \left( 1 - \frac{n_e(x, t)}{n_c} \right)^{1/2} \right] dx$$

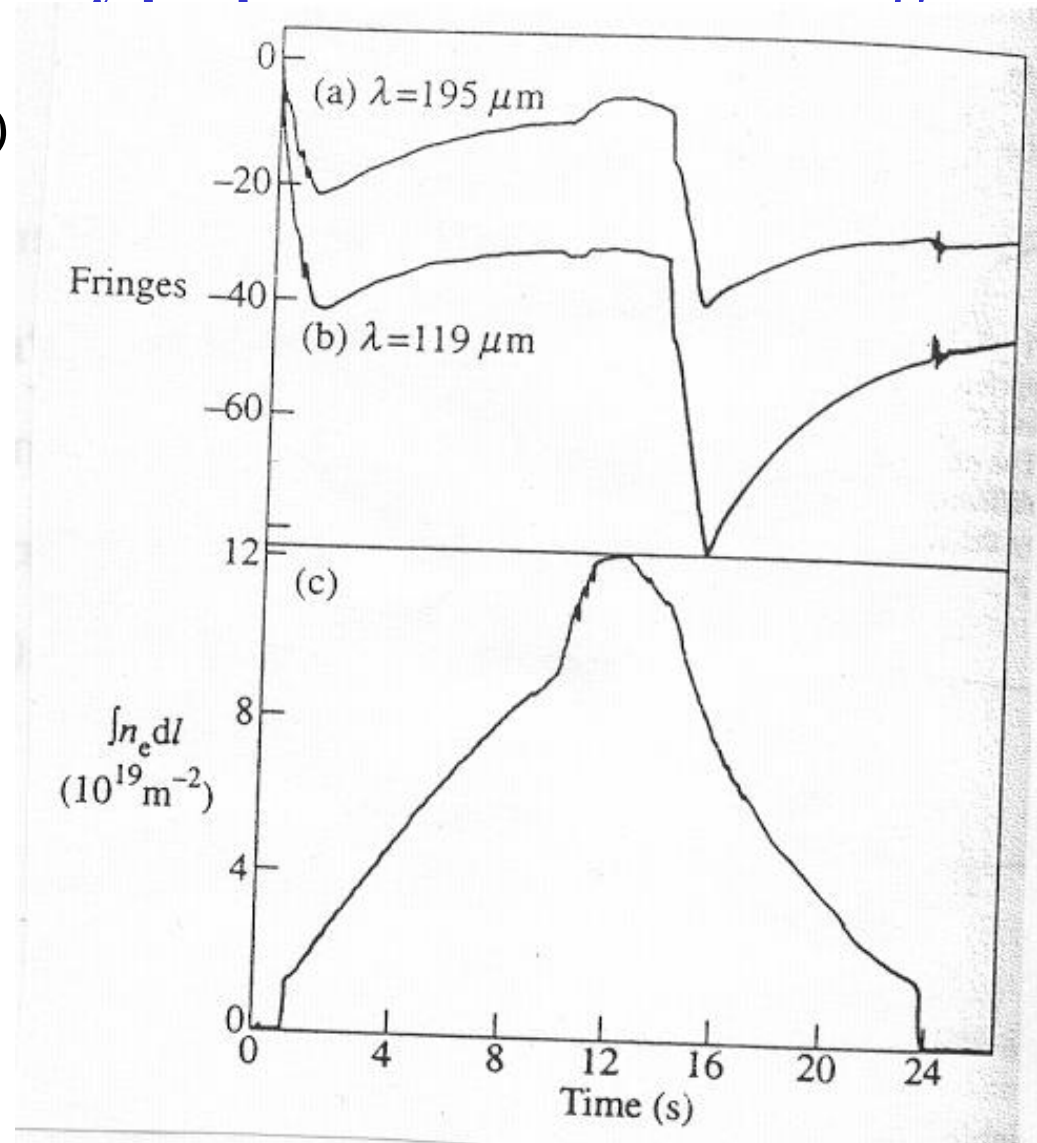
$$\Delta\phi(t) \approx \frac{\pi}{\lambda_0 n_c} \int n_e(x, t) dx \quad \text{for } n_e \ll n_c$$



# Two-Color Interferometry

**Mechanical vibration: inversely proportional to the wavelength**

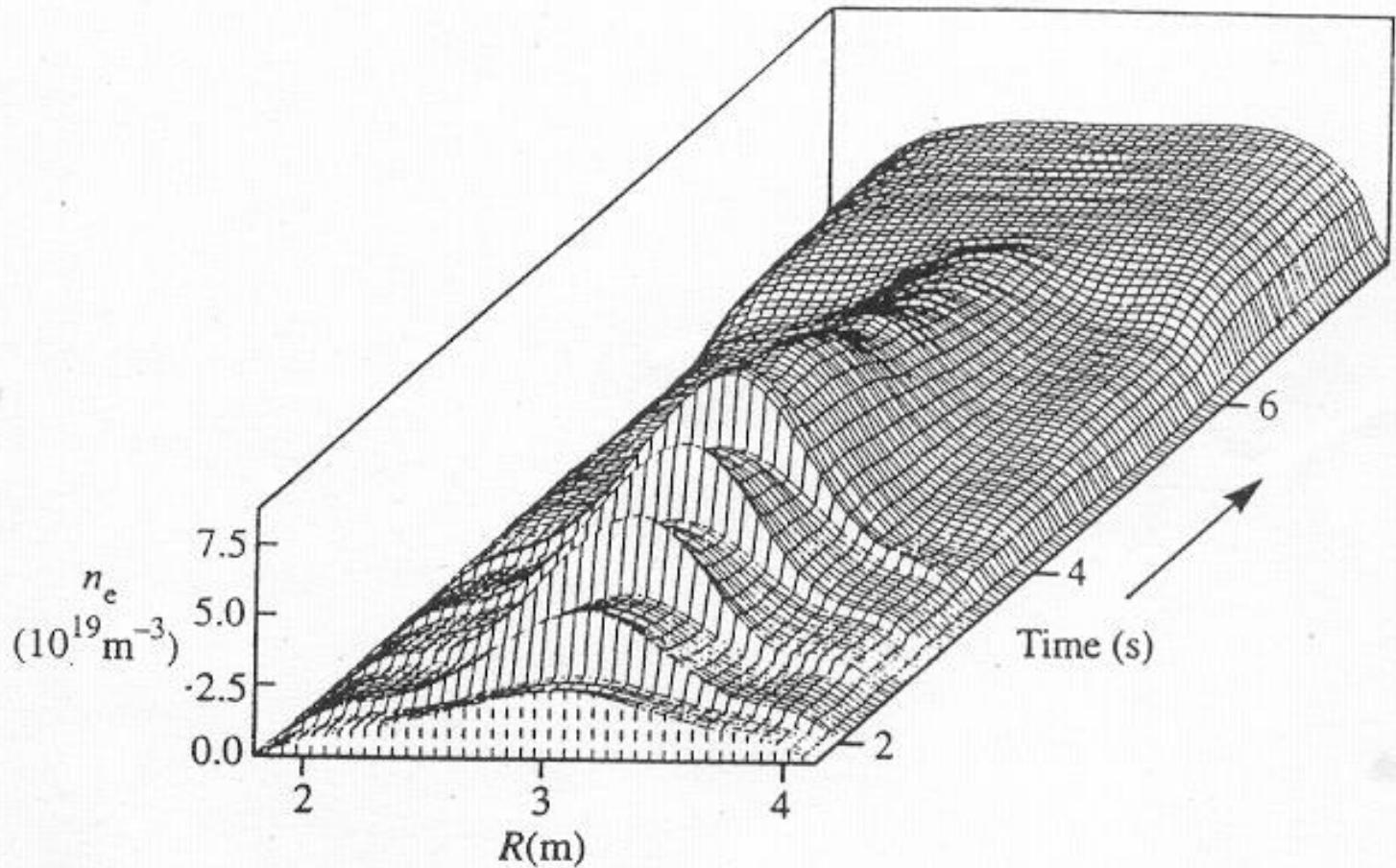
- JET ( $119\mu\text{m}$ ,  $195\mu\text{m}$ )
- C-Mod ( $10.6\mu\text{m}$ ,  $0.633\mu\text{m}$ )



# Inversion of Line-Integrated Density Profiles

**Abel inversion:**

$$n_e(r) = -\frac{1}{\pi} \int_r^a \frac{dN_e(x)}{dx} \frac{1}{(x^2 - r^2)^{1/2}} dx$$

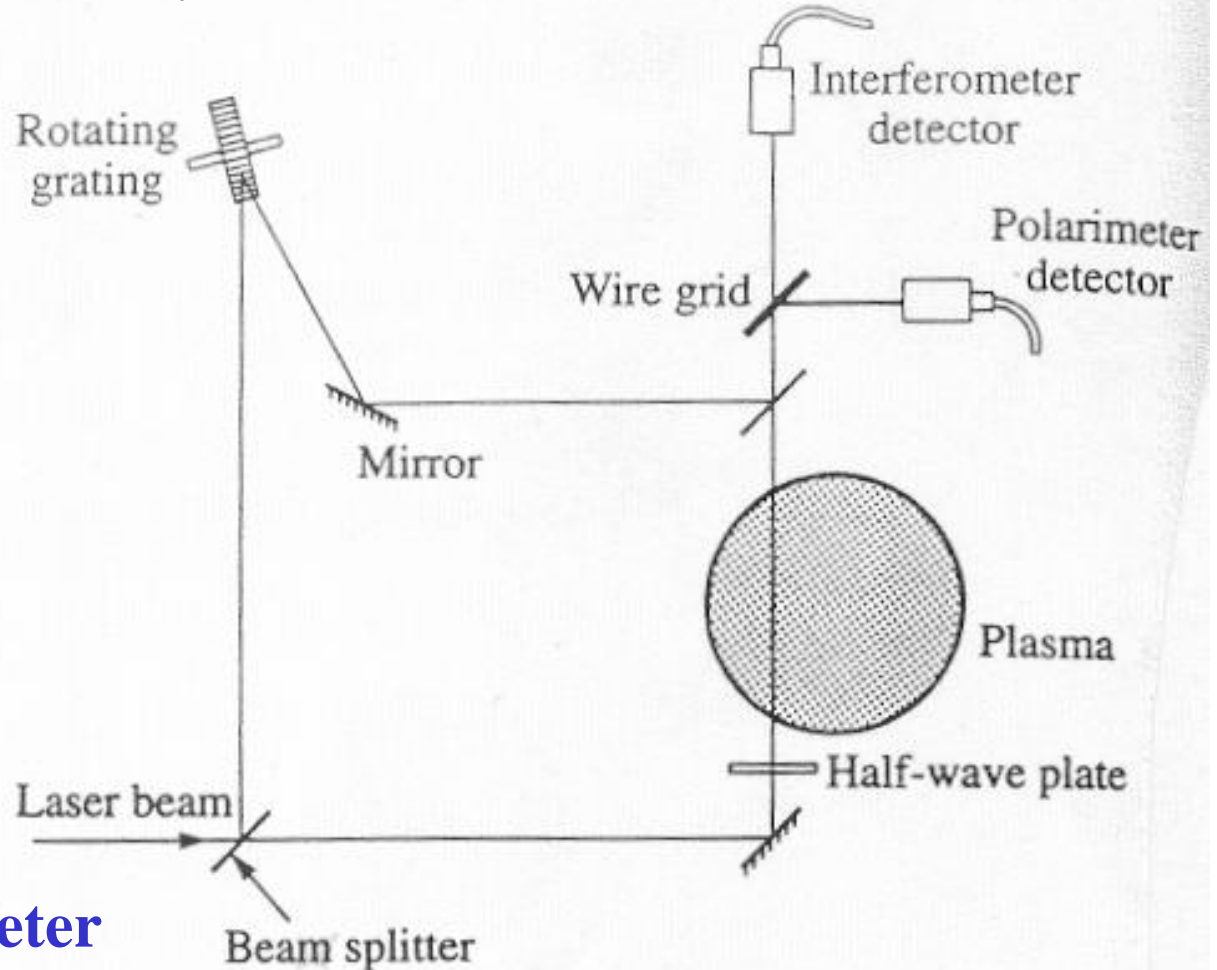


# Polarimetry: Faraday Rotation

Refractive index  $\mu_{\pm} = 1 - \frac{\omega_p^2}{\omega^2} \frac{\omega}{\omega \pm \omega_{ce}}$

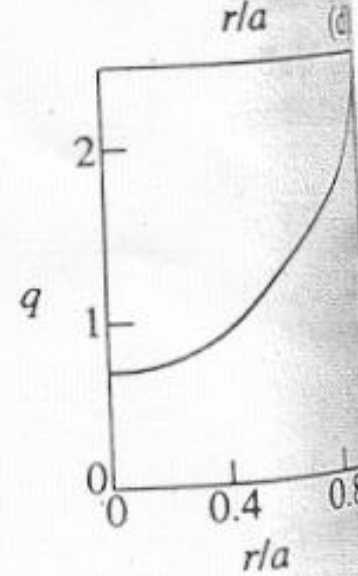
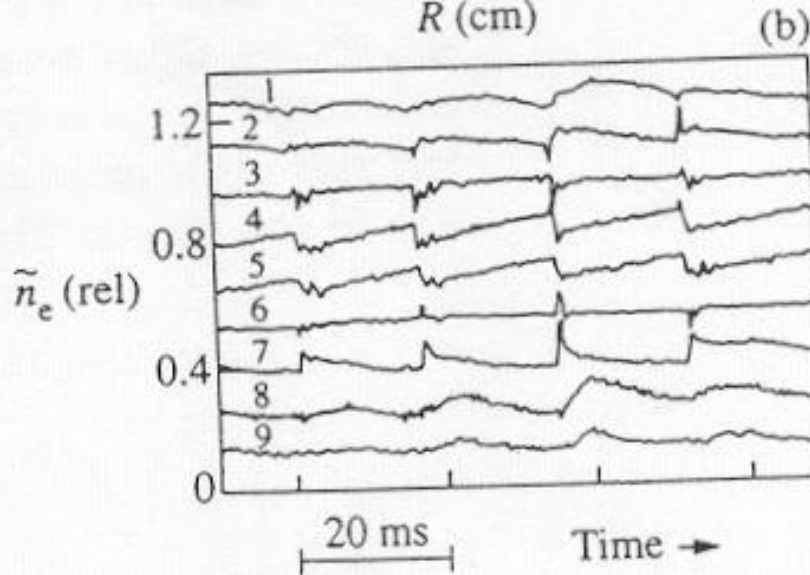
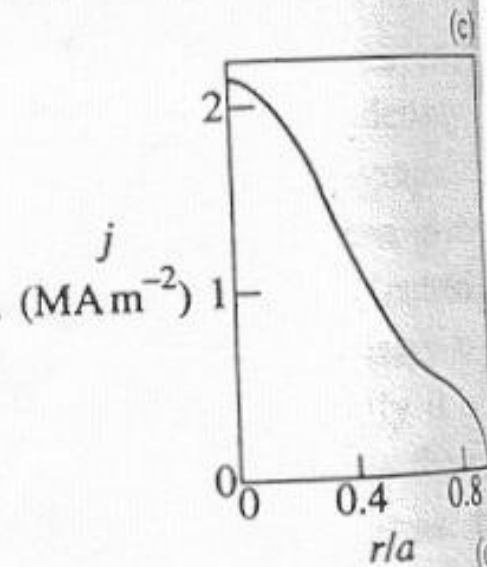
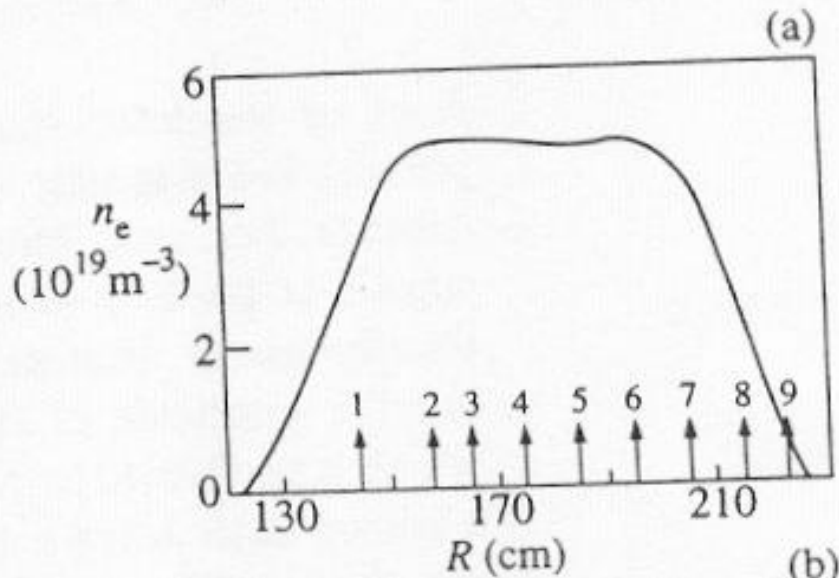
Rotation angle due to Faraday rotation

$$\theta_F = \frac{\lambda^2 e^3}{8\pi^2 \epsilon_0 m_e^2 c^3} \int n_e B_{\parallel} dl$$



**TEXTOR Polarimeter**

# Polarimeter Data for a Sawtoothing Plasma

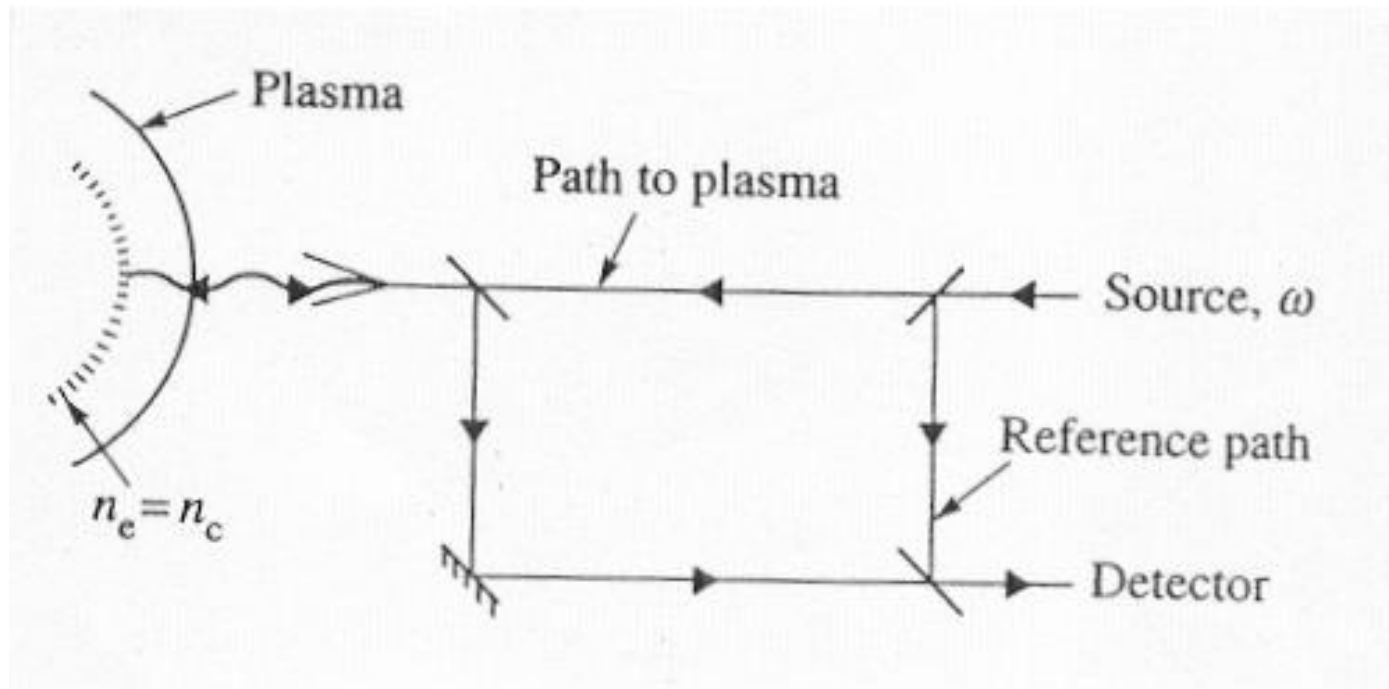


**TEXTOR**  
 $q_0 \sim 0.7$

# Reflectometry

The plasma density can be obtained by detecting the wave reflected at the cut-off positions. Different techniques are

- Linear frequency sweep
- Dual frequency differential phase
- Amplitude modulation
- Pulsed radar, pulse compression radar, noise correlation radar

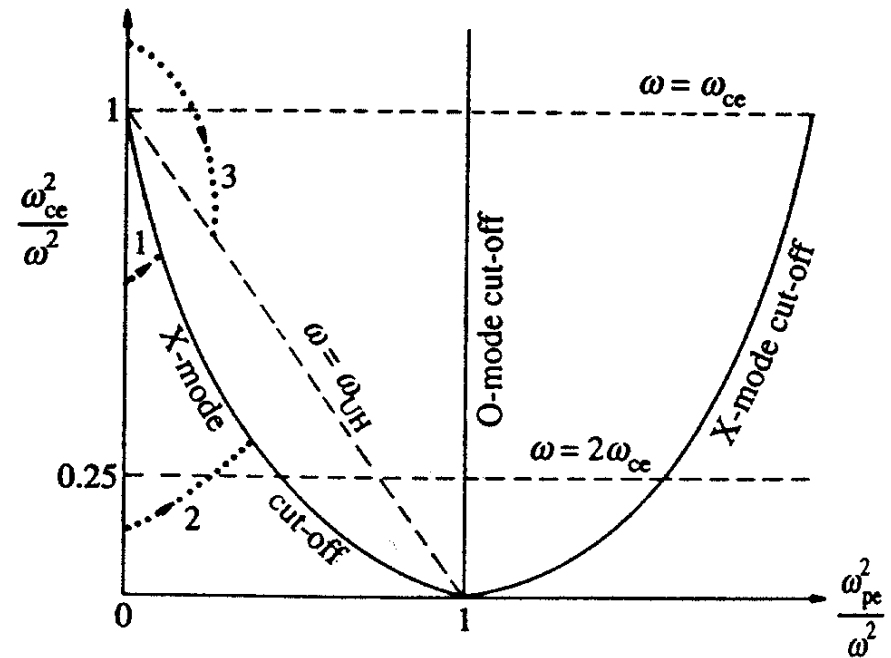
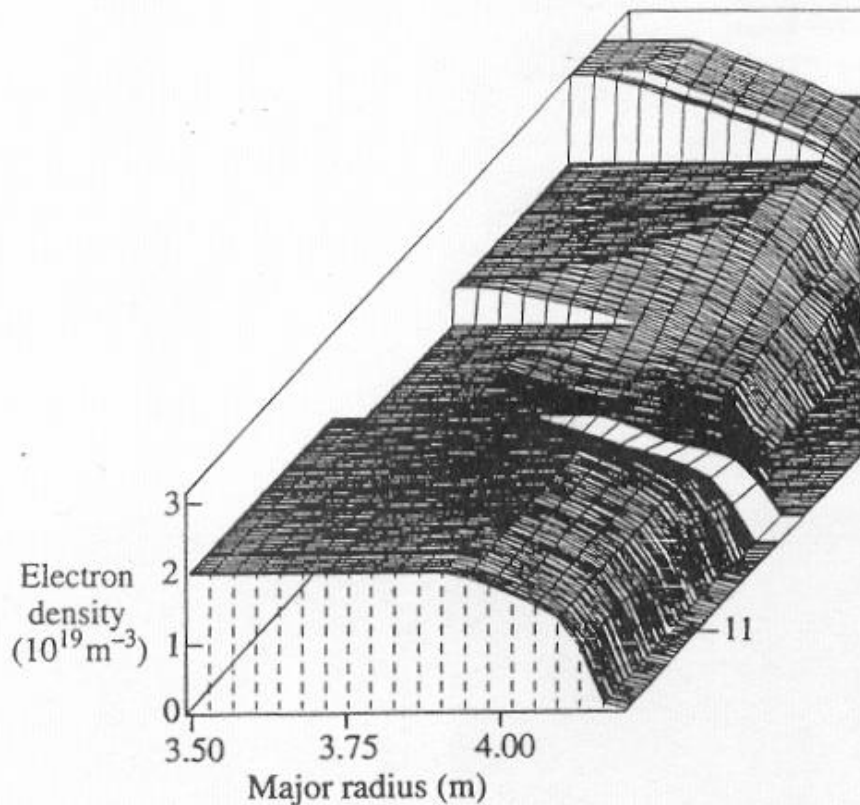


# Reflectometry

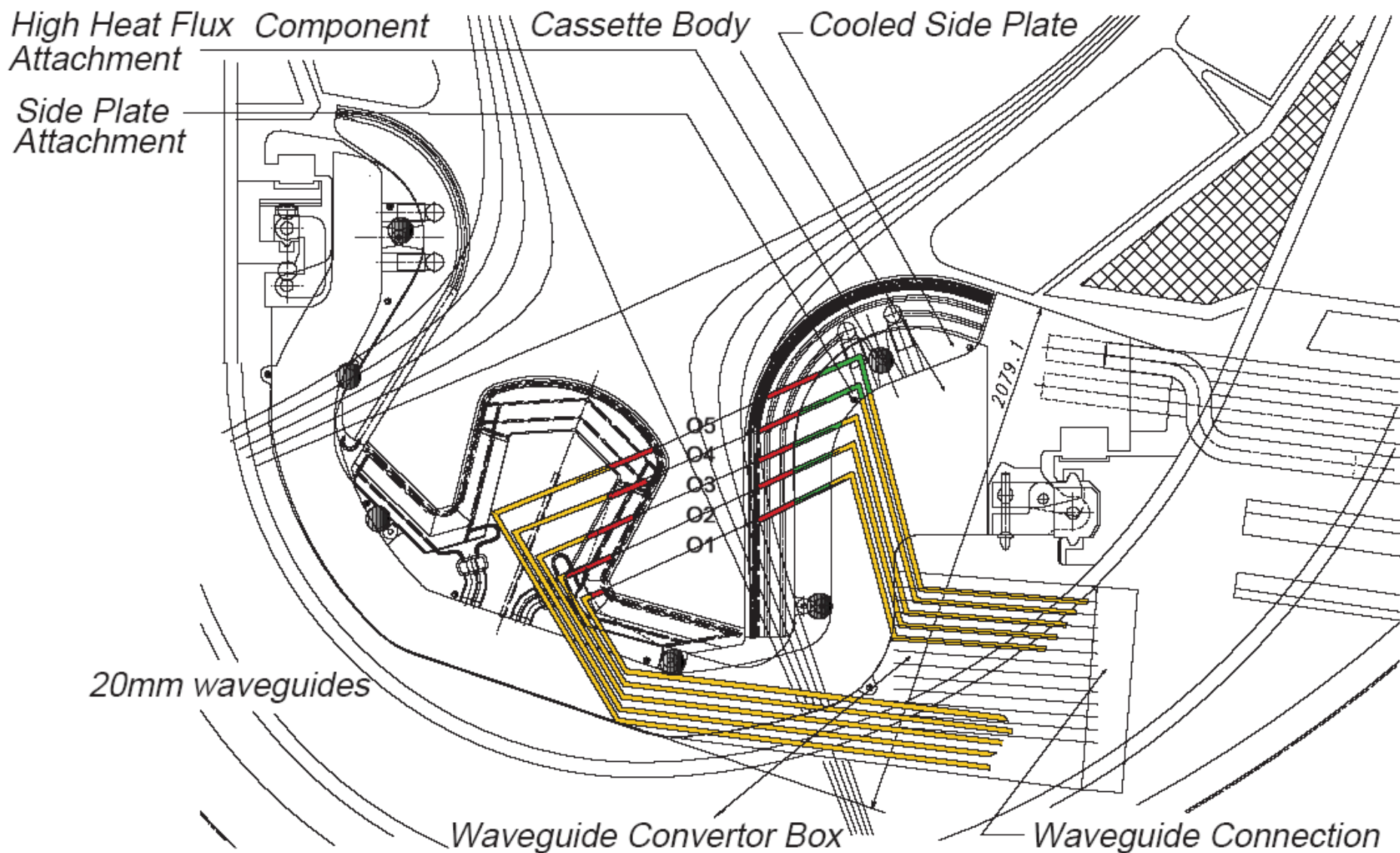
Accessibility makes reflectometry in two independent modes

- O-mode : cut-off at plasma frequency  $\omega = \omega_{pe} = (n_c e^2 / \epsilon_o m_e)^{1/2}$
- X-Mode: critical density depends also on magnetic field strength

$$\omega = \omega_{U,L} = \left( \frac{\omega_{ce}^2}{4} + \omega_{pe}^2 \right)^{1/2} \pm \frac{\omega_{ce}}{2}$$

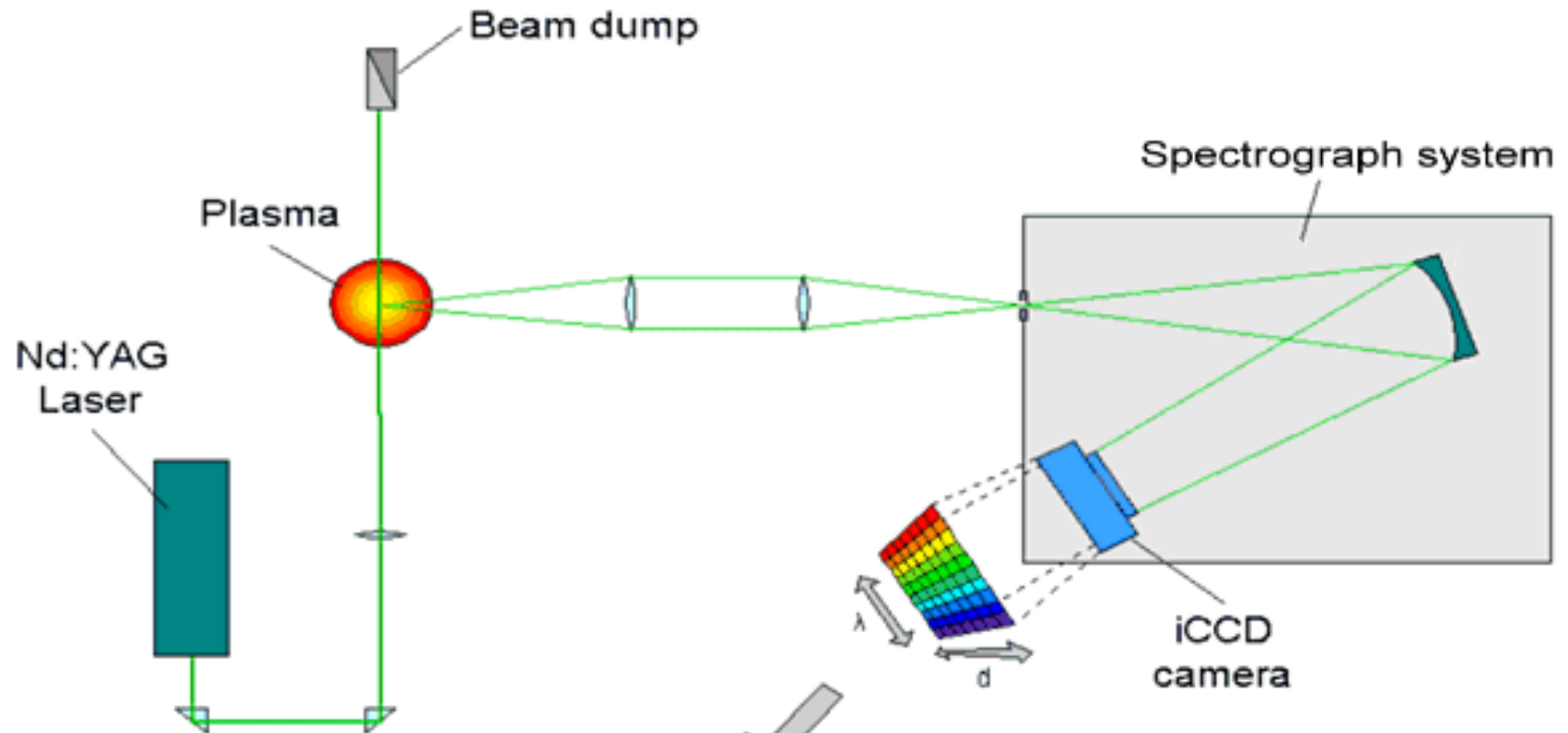


# ITER Divertor Interferometer/Reflectometry

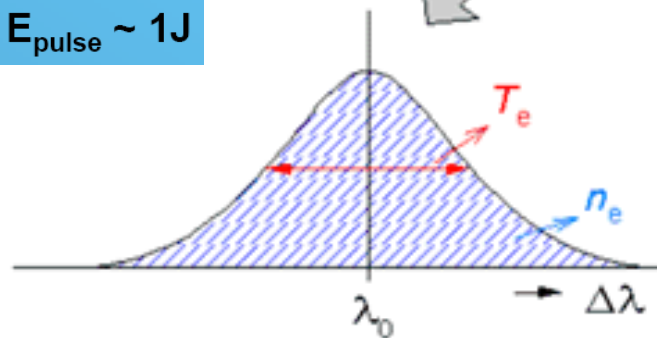




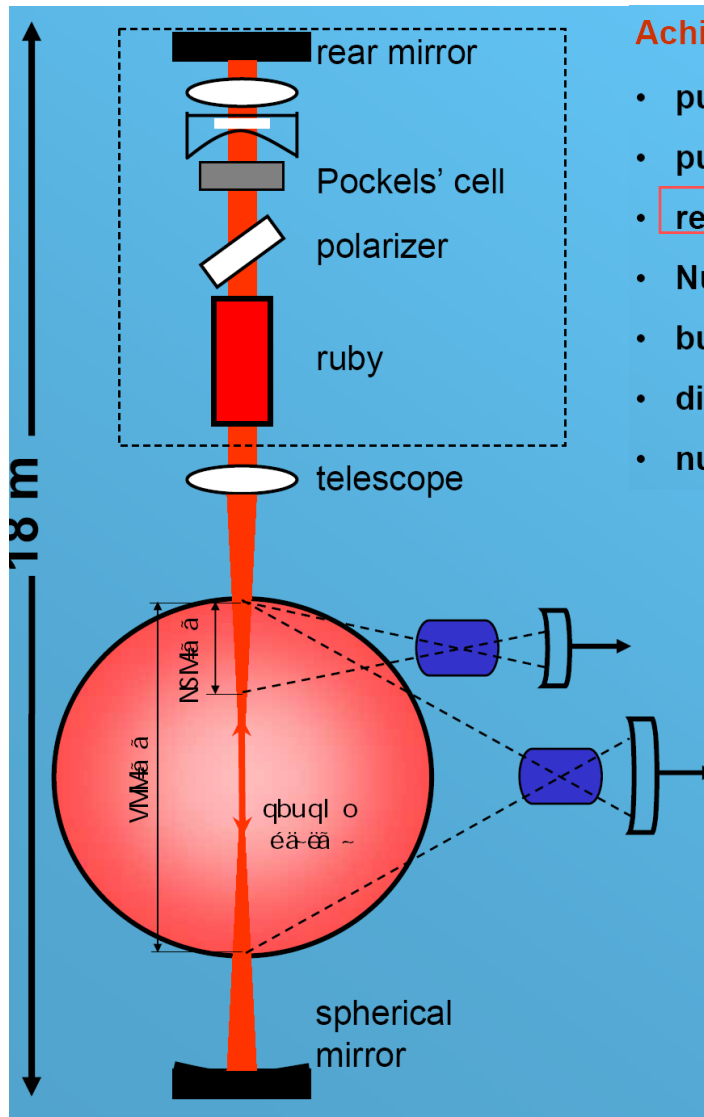
# Principle of Thomson Scattering



Nd:YAG lasers: 50 Hz,  $E_{\text{pulse}} \sim 1\text{J}$



# Multi-Pulse TEXTOR TVTS System



## Achieved specifications:

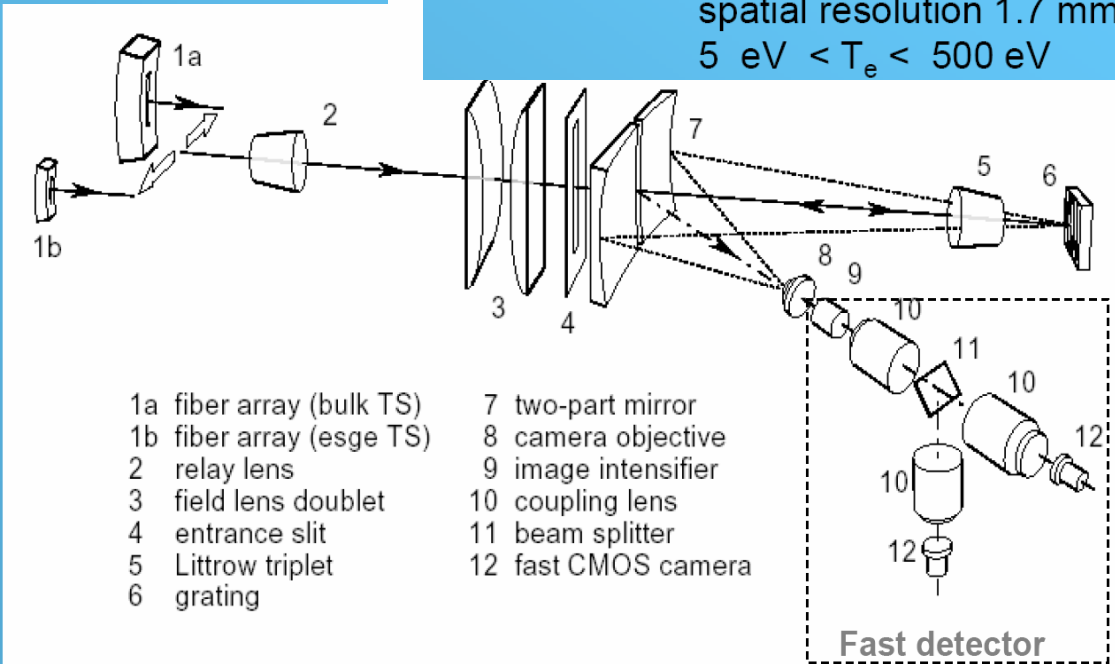
- pulse energy 12-15 J
- pulse width at FWHM 1  $\mu$ s
- rep. rate 5 kHz
- Number of pulses  $\sim$  20
- burst length  $\sim$  4 ms
- divergence  $\leq$  0.5 mrad
- number of bursts 1

## Fast repetitive high spatial resolution Thomson scattering system

- Fast repetitive high power laser
- Spectrometer equipped with fast detector

**Full chord TS:**  $-450 \text{ mm} < z < +450 \text{ mm}$   
 spatial resolution 7.5 mm  
 $50 \text{ eV} < T_e < 5 \text{ keV}$

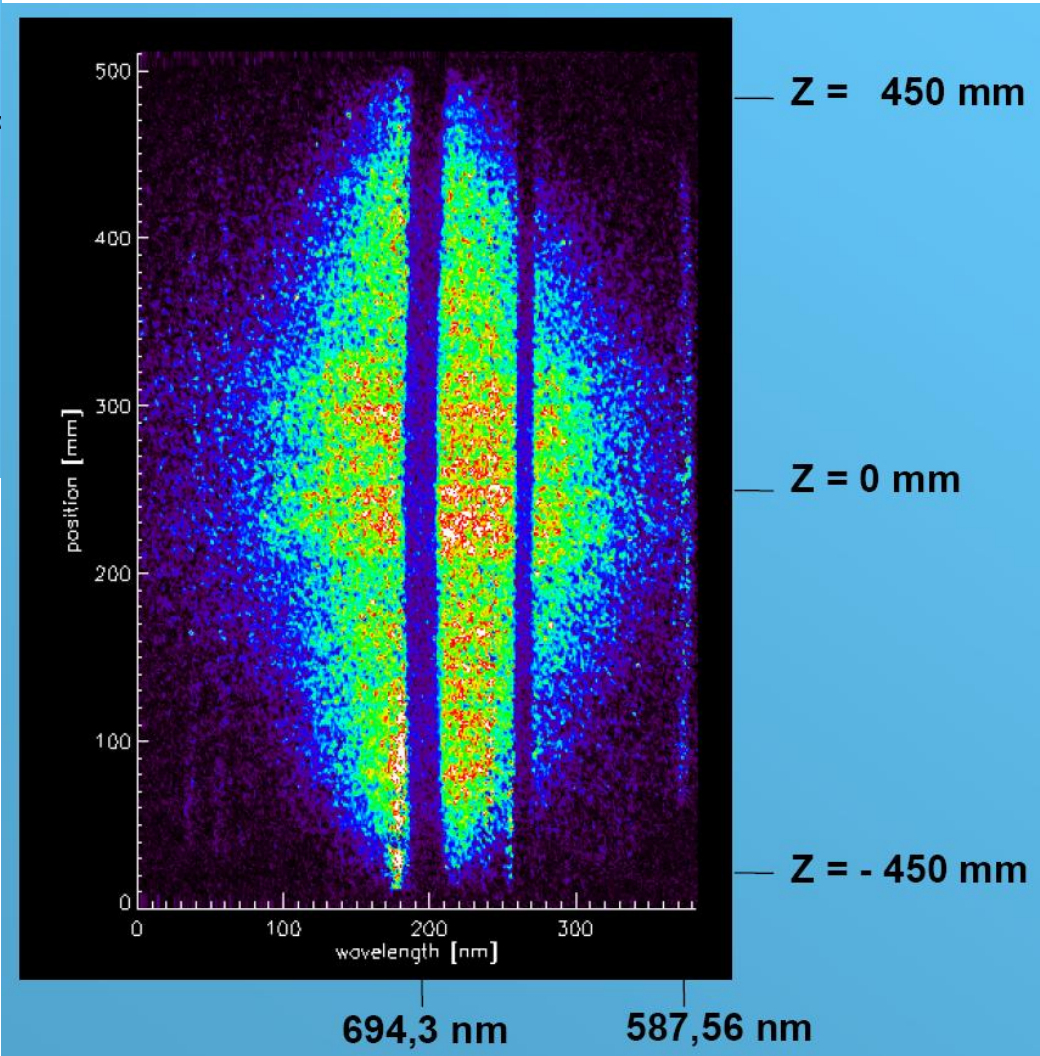
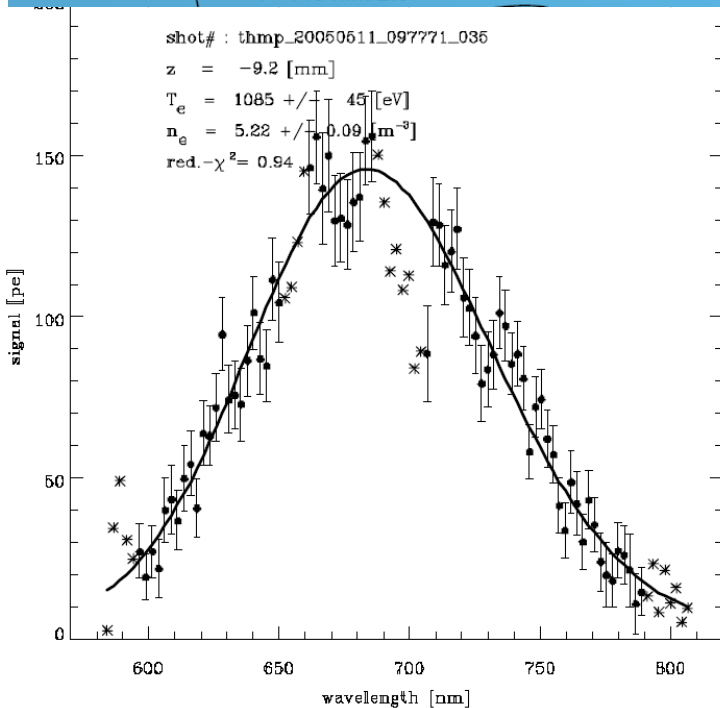
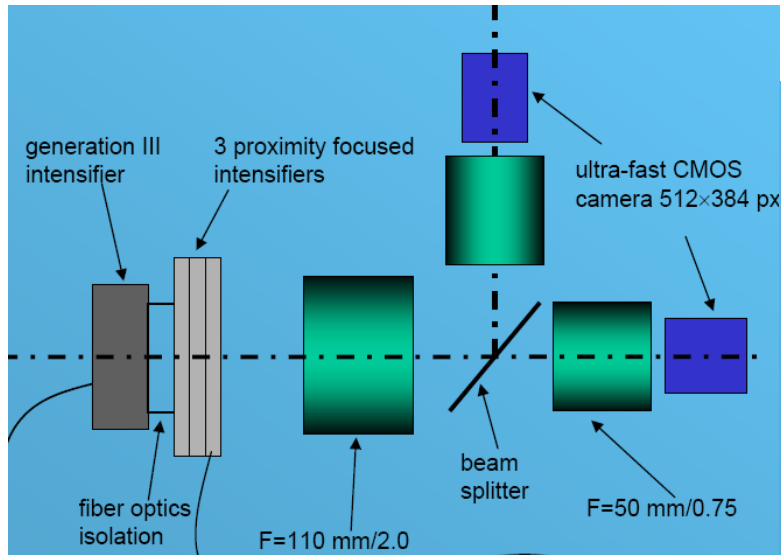
**Edge TS:**  $+340 \text{ mm} < z < +500 \text{ mm}$   
 spatial resolution 1.7 mm  
 $5 \text{ eV} < T_e < 500 \text{ eV}$



- |                          |                     |
|--------------------------|---------------------|
| 1a fiber array (bulk TS) | 7 two-part mirror   |
| 1b fiber array (esge TS) | 8 camera objective  |
| 2 relay lens             | 9 image intensifier |
| 3 field lens doublet     | 10 coupling lens    |
| 4 entrance slit          | 11 beam splitter    |
| 5 Littrow triplet        | 12 fast CMOS camera |
| 6 grating                |                     |

Fast detector

# TEXTOR TVTS System



# JET LIDAR Thomson Scattering

1J ruby laser (wavelength 694nm)

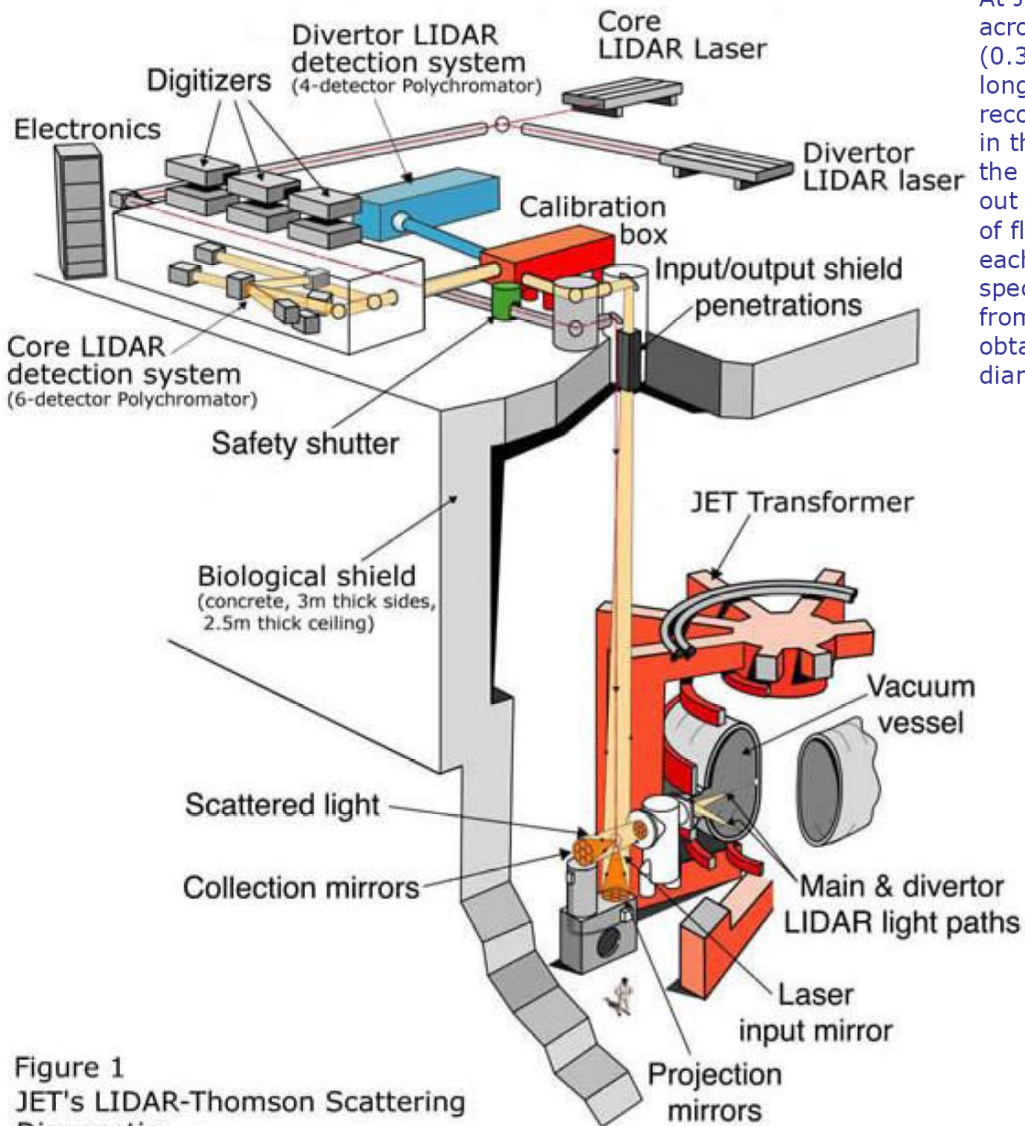
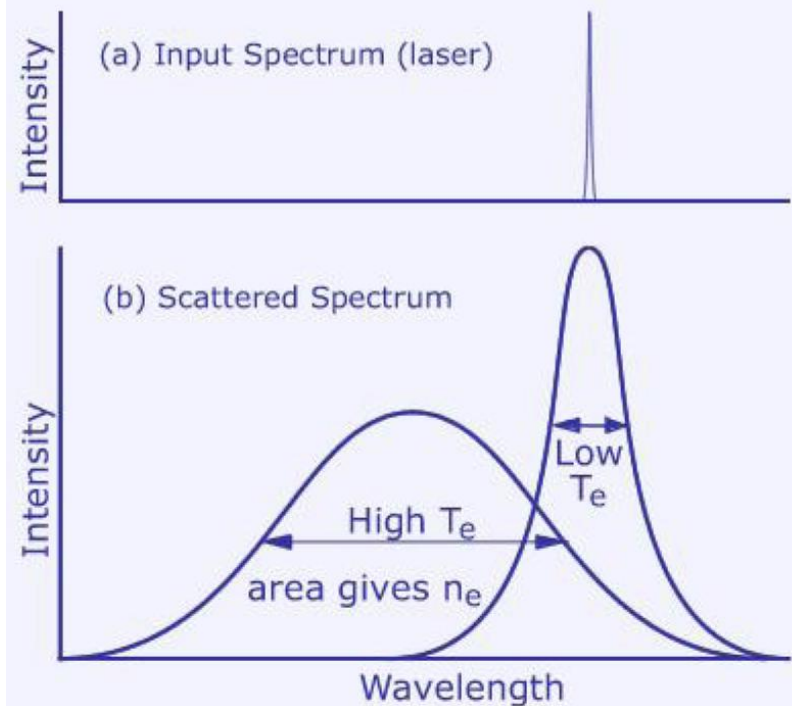


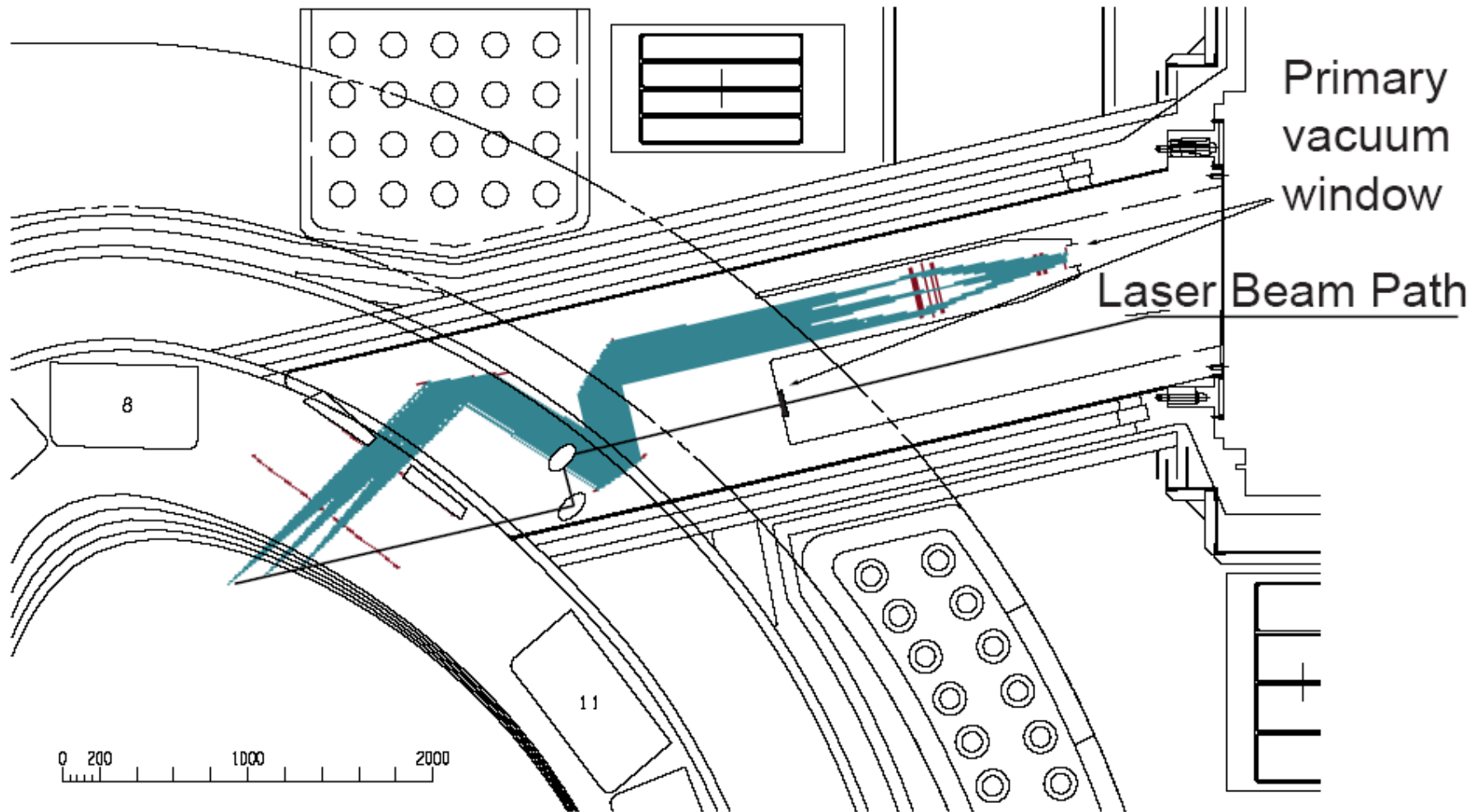
Figure 1  
JET's LIDAR-Thomson Scattering Diagnostic

At JET we also want to know how the temperature and density vary across the plasma. To get this information we send a short laser pulse (0.3 nano-seconds duration which, at the speed of light, is only 10 cm long) across the plasma diameter. By using a fast detection and recording system, we can observe its progress by capturing the changes in the back-scattered spectrum. We can then analyse these changes as the pulse passes from the relatively cool edge, through the hot core and out again through the opposite plasma edge. Since we know by the time of flight, or LIDAR, principle where the laser pulse is in the plasma at each instant, we can compute from the instantaneous scattered spectrum the local values of temperature and density in the plasma, i.e. from the time of flight of one laser pulse through the plasma we can obtain the temperature and density variations across the whole diameter.

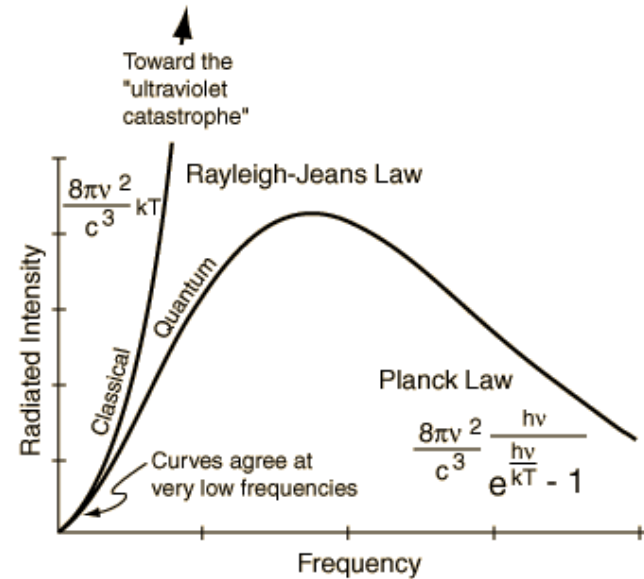
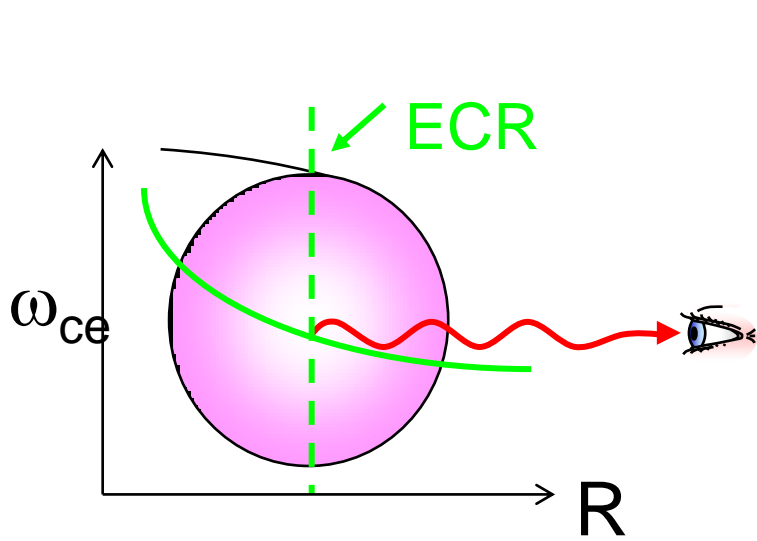
Figure 2 Input and Scattered Spectra



# ITER Thomson Scattering System



# Electron Cyclotron Emission (ECE)



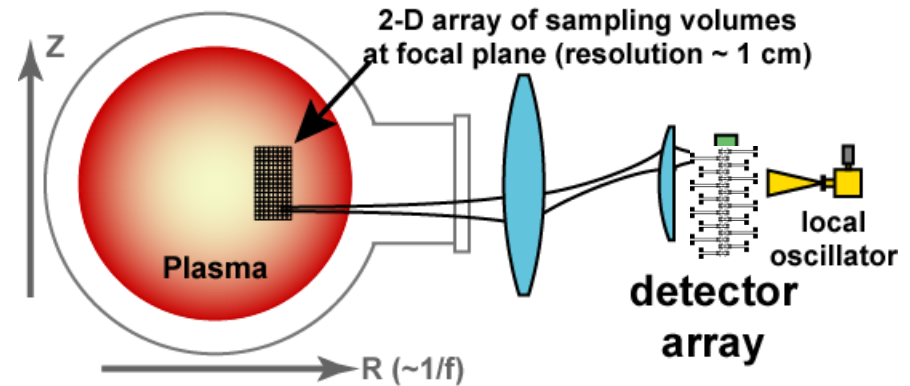
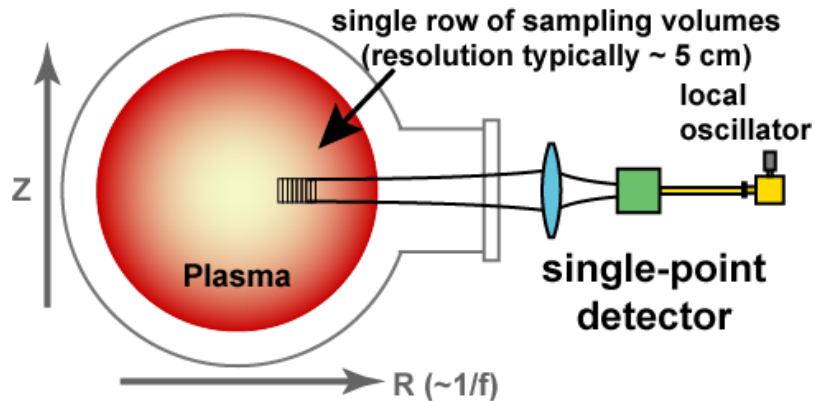
- Electromagnetic (EM) waves are emitted at the electron cyclotron resonance (ECR) layer at a series of discrete harmonic frequencies:

□  $\omega_n = n\omega_{ce}$  ,  $\omega_{ce}(R) \propto \mathbf{B} \propto 1/R$

- If the plasma is Maxwellian and optically thick, the emission can be described as blackbody radiation in the Rayleigh-Jens law

– Intensity:  $I(\omega) = I_B(\omega) \approx \frac{T_e \omega^2}{8\pi^3 c^2}$

# 2D ECE Imaging System

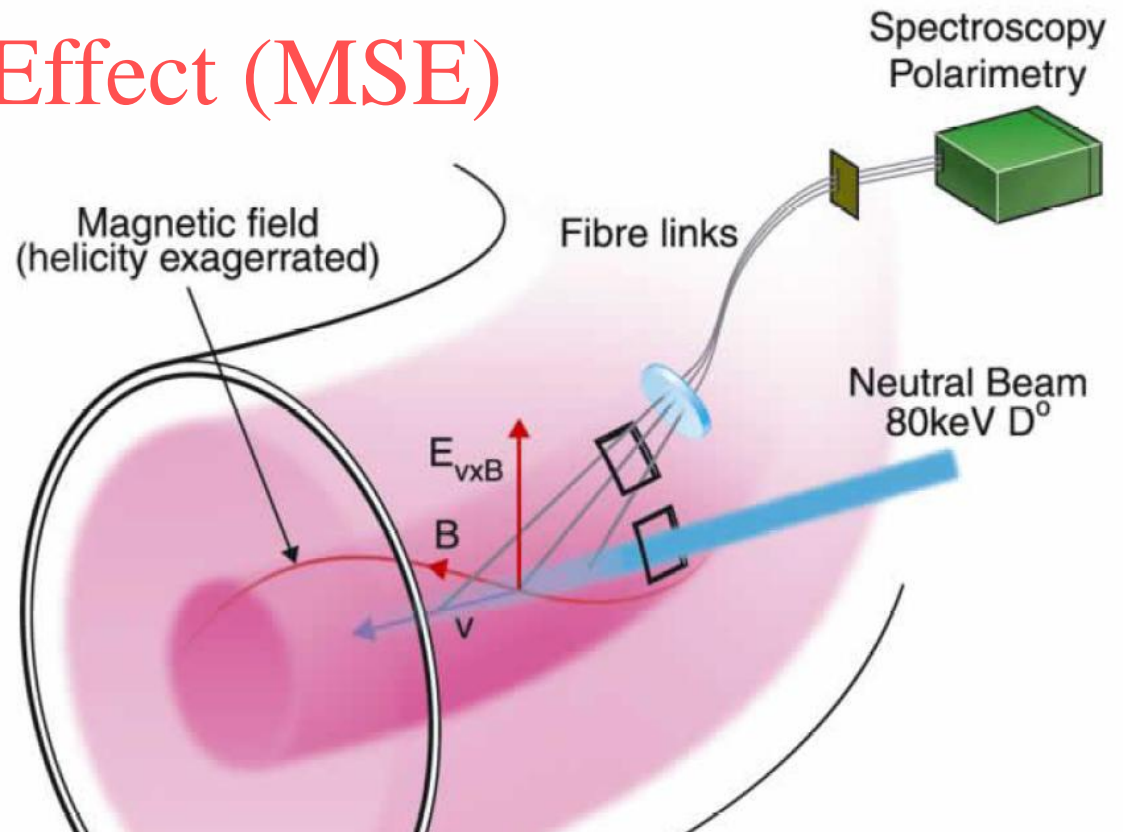


## Conventional 1-D ECE system

## 2-D ECE imaging system

- ECE measurement is an established tool for electron temperature measurement in high temperature plasmas
- Sensitive 1-D array detector, imaging optics, and wide-band mm wave antenna, and IF electronics are required for 2-D imaging system
- $T_e$  fluctuation measurement
  - Real time fluctuations can be studied up to  $\sim 1\%$  level
  - Fluctuation studies down to  $0.1\%$  level have been performed using long time integration

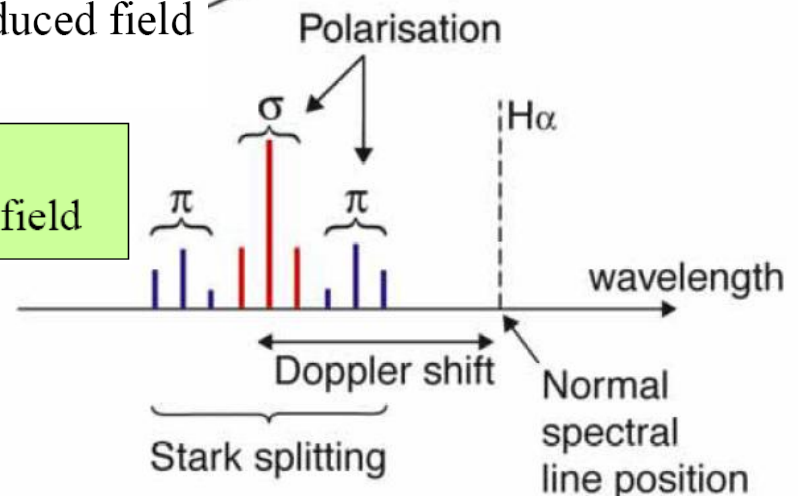
# Motional Stark Effect (MSE)



$$\underbrace{\mathbf{E}}_{\text{measured}} = \underbrace{\mathbf{V}}_{\text{known from DNB}} \times \underbrace{\mathbf{B}}_{\text{unknown}}$$

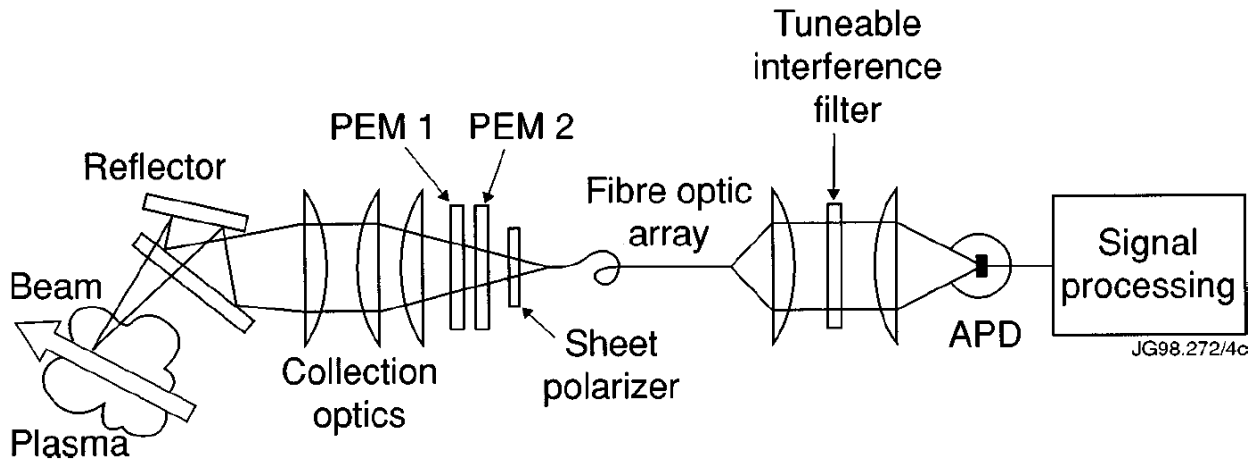
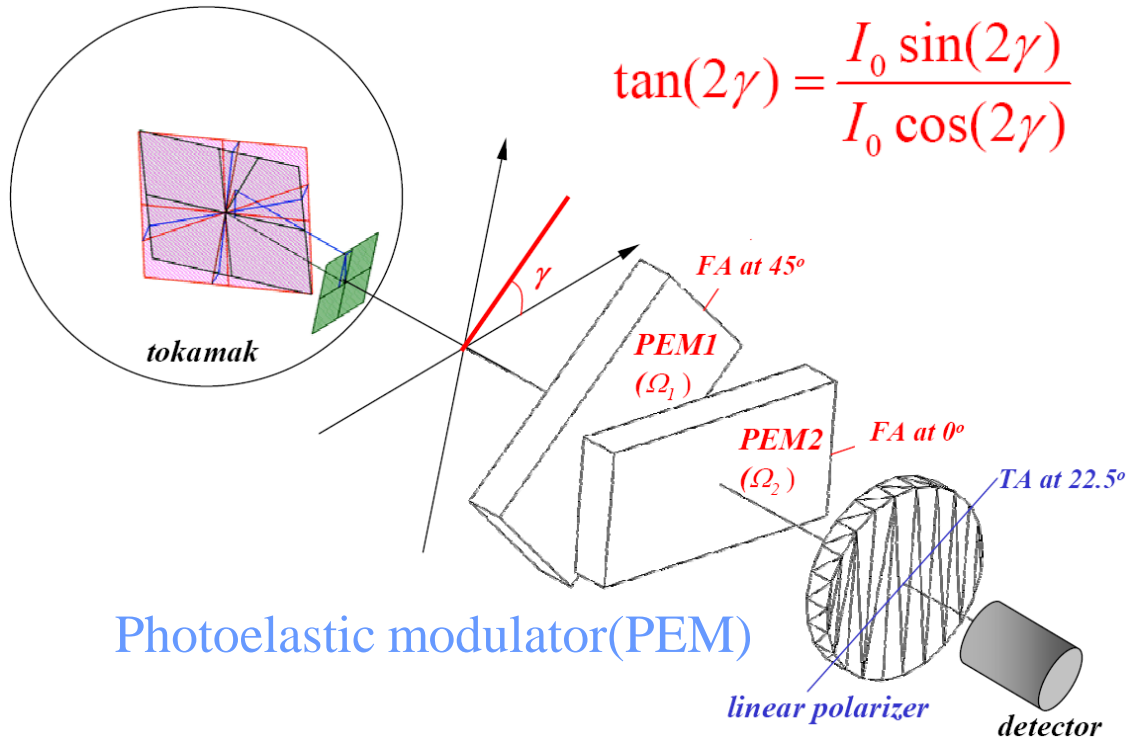
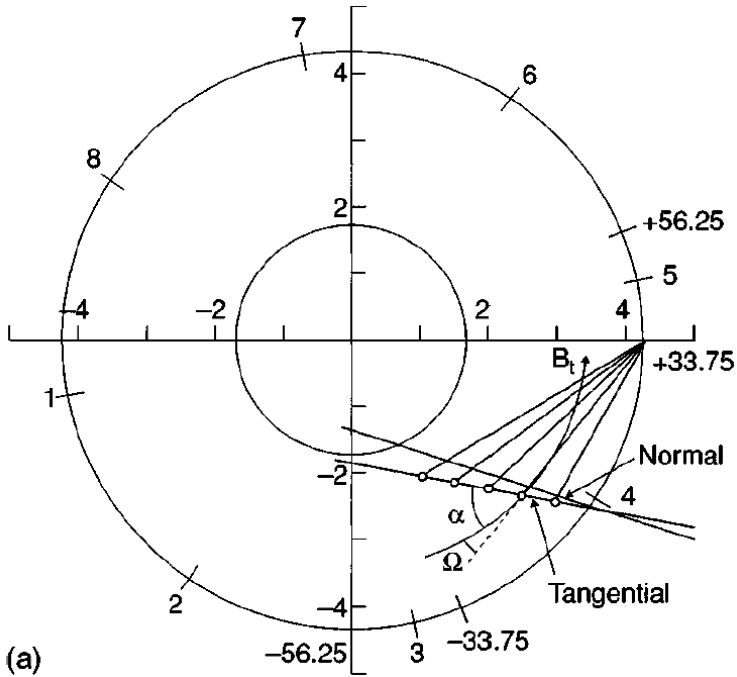
♣ If we can measure the polarization angle of the  $\sigma$  (or  $\pi$ ) components in the Stark spectra with respect to the induced field  $E$ , we can know **the direction of  $B$**  (pitch angle)

**$\pi$  components** : polarized **parallel** to the local  $E$  field  
 **$\sigma$  components** : polarized **perpendicular** to the local  $E$  field

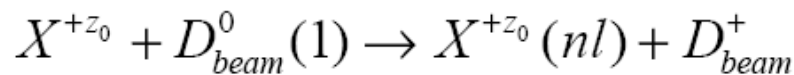
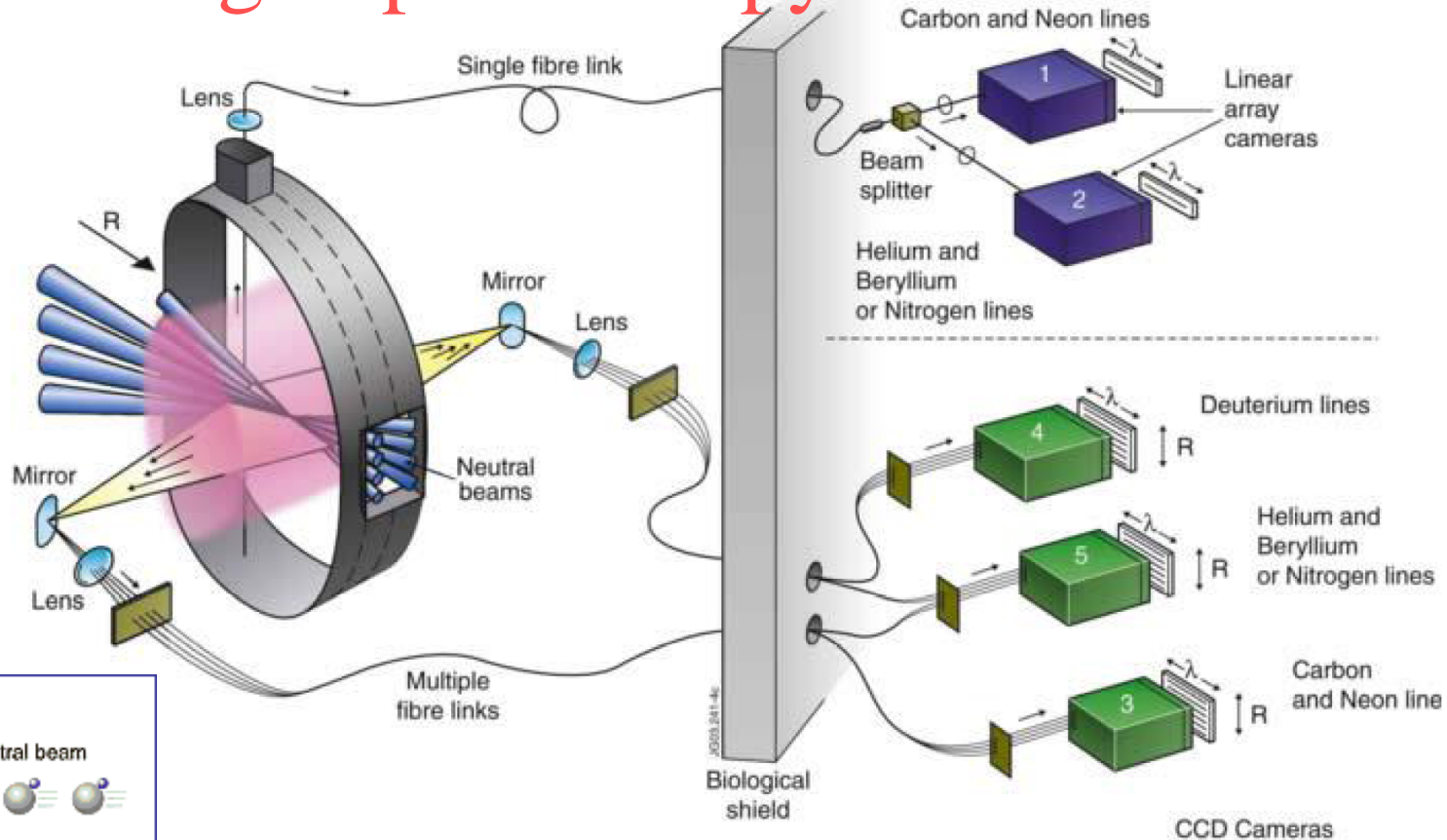




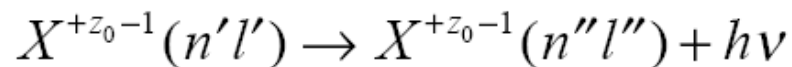
# Motional Stark Effect (MSE)



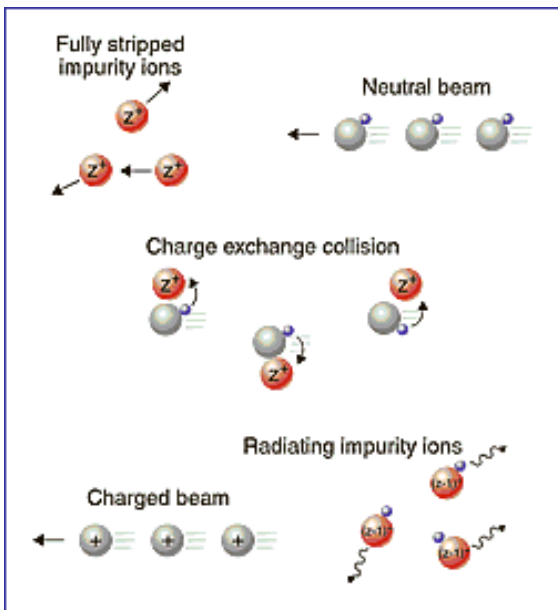
# Charge Exchange Spectroscopy



Subsequently the hydrogen-like impurity ion radiates as



densities of fully stripped low-Z ions and ion temperatures and plasma rotation



# Beam Emission Spectroscopy (BES)

To obtain two-dimensional measurements of density fluctuations in the confined regions of hot plasmas, the Beam Emission Spectroscopy (BES) diagnostic system has been utilised on a number of US tokamaks, such as DIII-D, NSTX, etc. The BES diagnostic system measures local, long wavelength density fluctuations by observing the fluorescence of the ITER diagnostic neutral beam. BES measures density fluctuations by observing the Doppler-shifted  $D_\alpha$  emission. Fluctuations in the light emission intensity are proportional to the local density fluctuations that depend on the local plasma density, temperature, beam energy and  $Z_{\text{eff}}$ . The optical viewing sightlines are deployed so that they are nearly tangent to a magnetic flux surface at the intersection point with the neutral beam volume to achieve good radial and poloidal resolution.

# Heavy Ion Beam Probe (HIBP)

heavy ion beam diagnostic (HIBD) as a candidate to perform the measurements of the  $B_p$  and  $E_r$  edge profiles in the ITER.

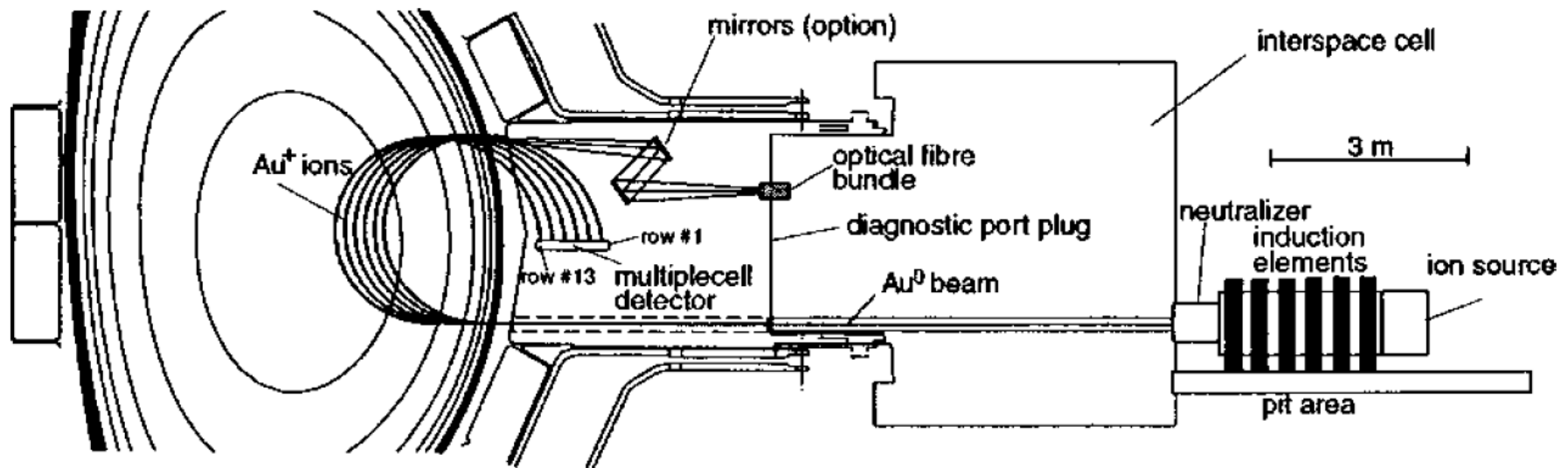


FIG. 2. Schematic layout of a HIBD for the ITER based on the injection of a  $\text{Au}^0$  neutral beam. The  $\text{Au}^+$  probing ions are collected in a matrix multiple cell detector. Also shown is an optional optical arrangement which can be used for imaging the emission light from the individual  $\text{Au}^+$  beams into a spectrometer for measuring the ions speed.

# X-ray Spectroscopy

- **High resolution X-ray spectroscopy has made invaluable contributions** to tokamak experiments by providing data on the **central ion and electron temperatures,  $T_i(0)$  and  $T_e(0)$ , the central toroidal plasma rotation,  $v_t(0)$ , and the ionization equilibrium.** *It has also been important for experimental verifications of atomic theories and interpretation of stellar flares.*

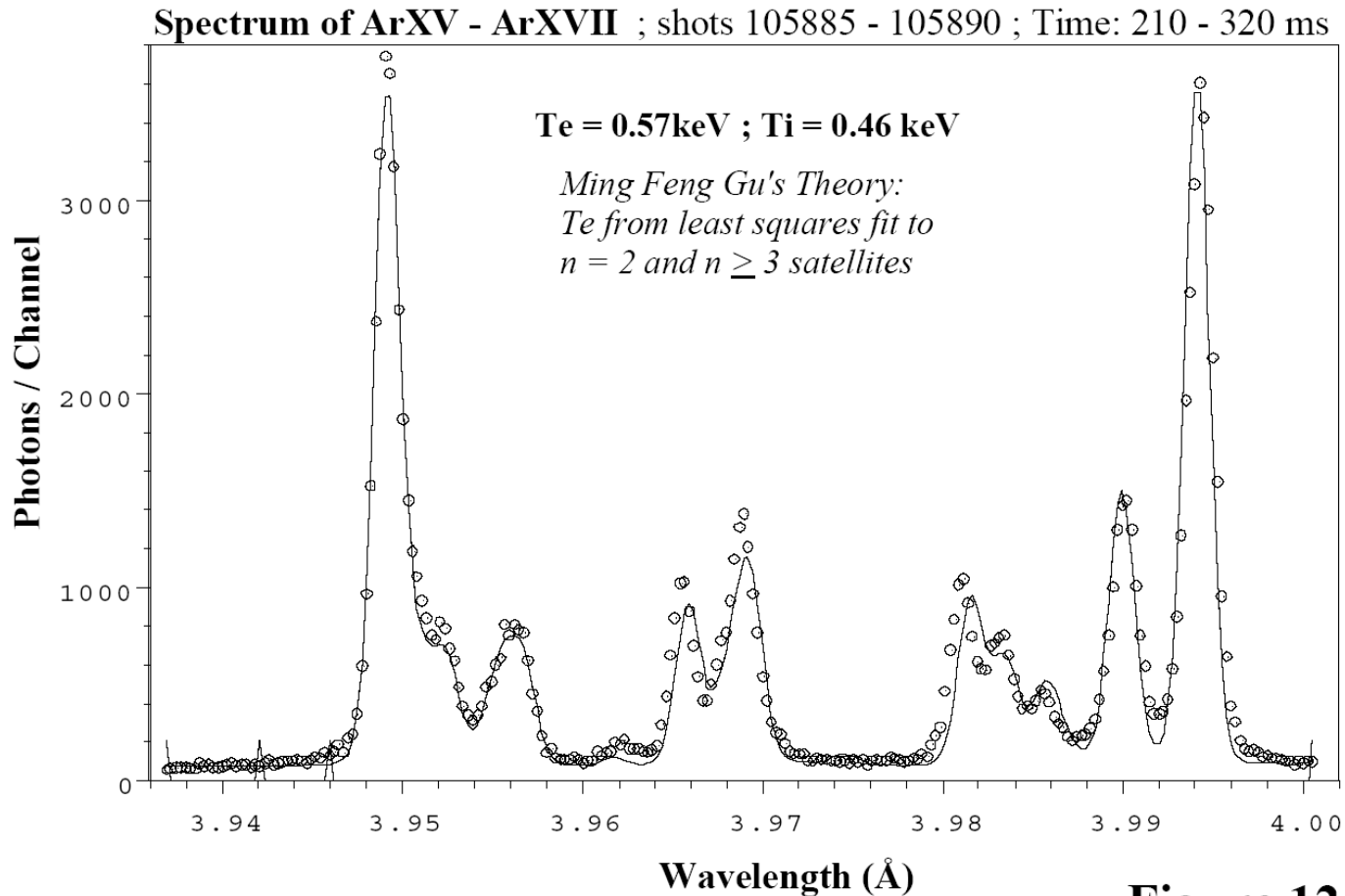
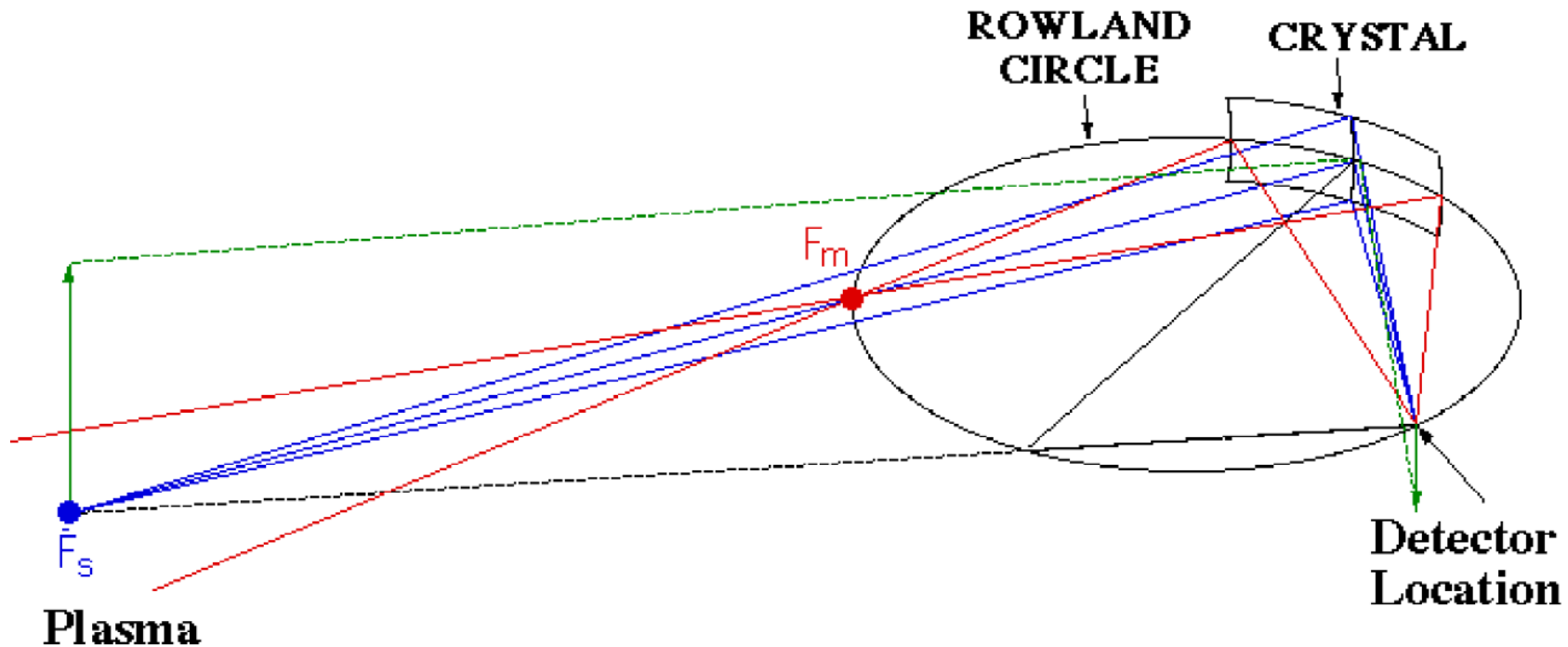


Figure 12

# X-ray Imaging Crystal Spectroscopy

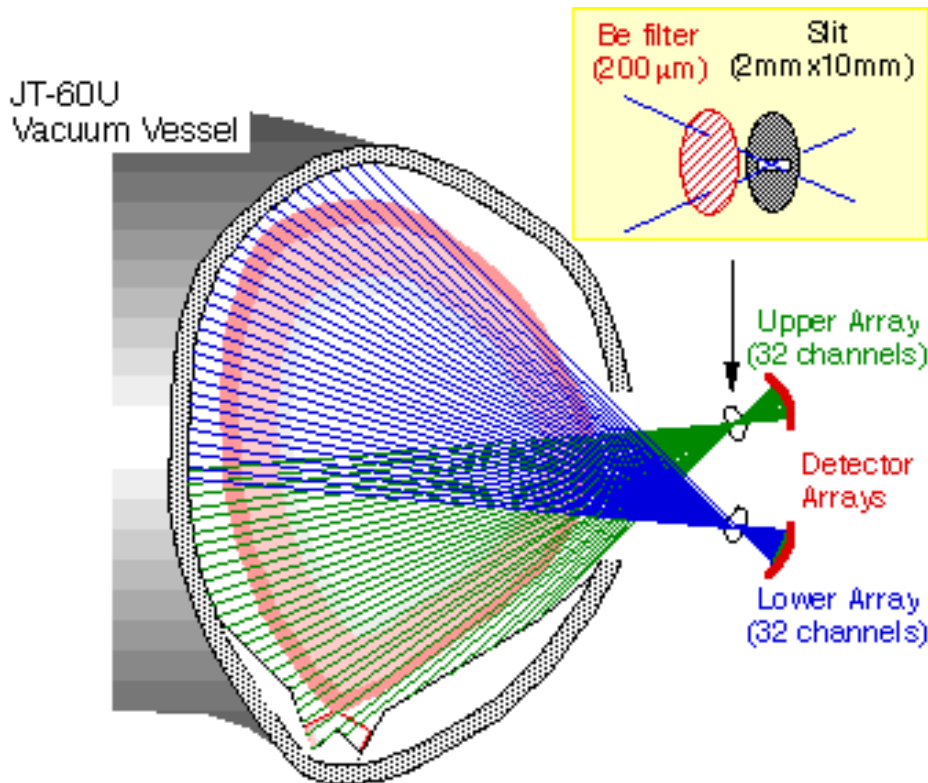


## Parameters of the upgraded X-ray Imaging Crystal Spectrometer

- **Crystal:**  
spherically bent circular 110-quartz crystal:  $2d = 4.913 \text{ \AA}$   
radius of curvature  $R_c = 375 \text{ cm}$   
crystal disc diameter  $d = 8 \text{ cm}$
- **Bragg angles for Lines of ArXVII:**  $53.5 < \theta < 54.5 \text{ degrees}$

# Soft X-ray Array

To observe collective behavior (density, temperature etc.) of electrons and magnetohydrodynamic activity in a high temperature plasma



A schematic picture of viewing lines of upper and lower detector arrays.

[Detectors, Diagnostic Method]  
Soft X-rays emitted as bremsstrahlung by free electrons in a plasma are detected by PIN diodes and a Beryllium (Be) filter with 200 μm thickness. Bremsstrahlung is a function of electron density, temperature, and impurity contamination and is sensitive to electron temperature in the energy range of the soft X-ray. Evolution of the soft X-ray intensity profile suggests the collective motion of electrons or magnetohydrodynamic activity in a plasma.

[Specifications]

Time resolution : 80 ms

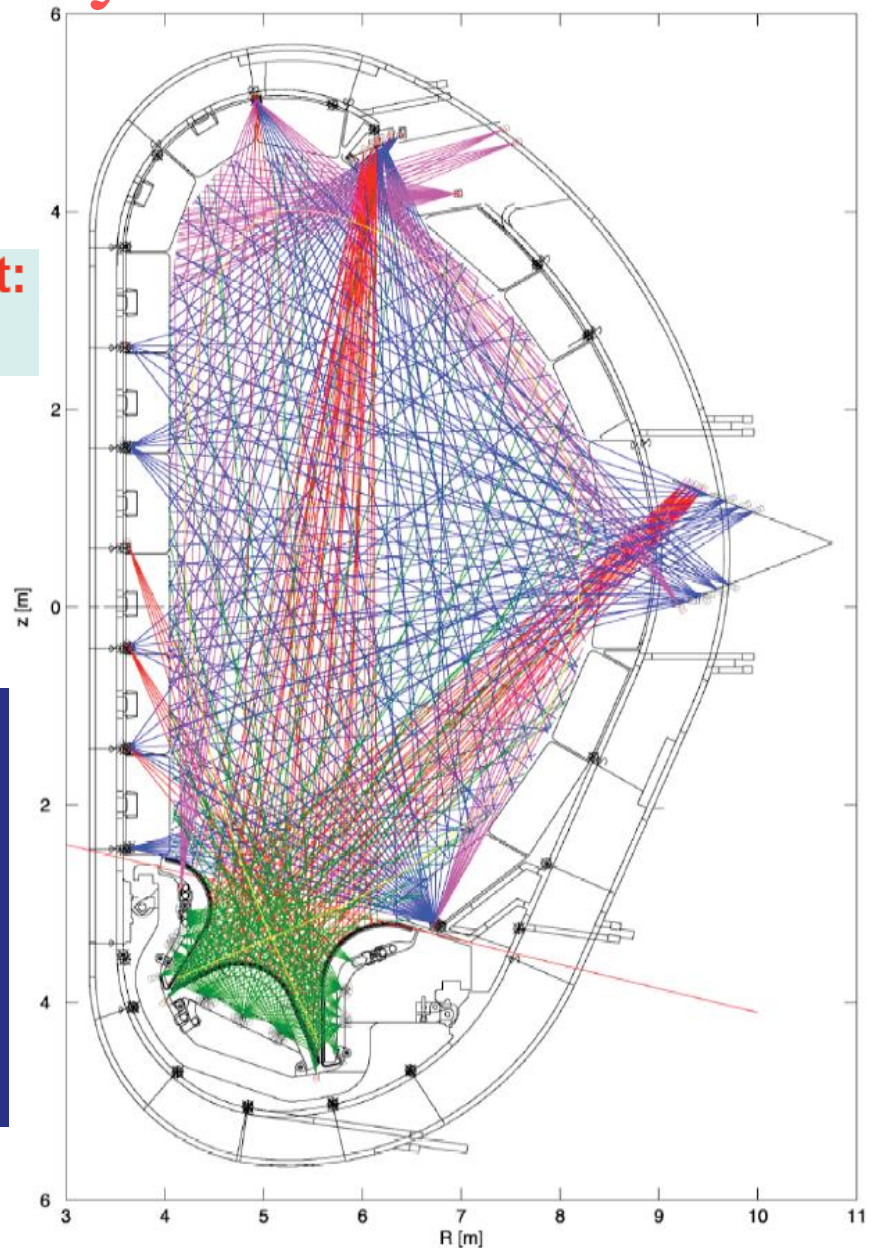
Spatial resolution: 3 - 5 cm

# Bolometry

## ITER Bolometry

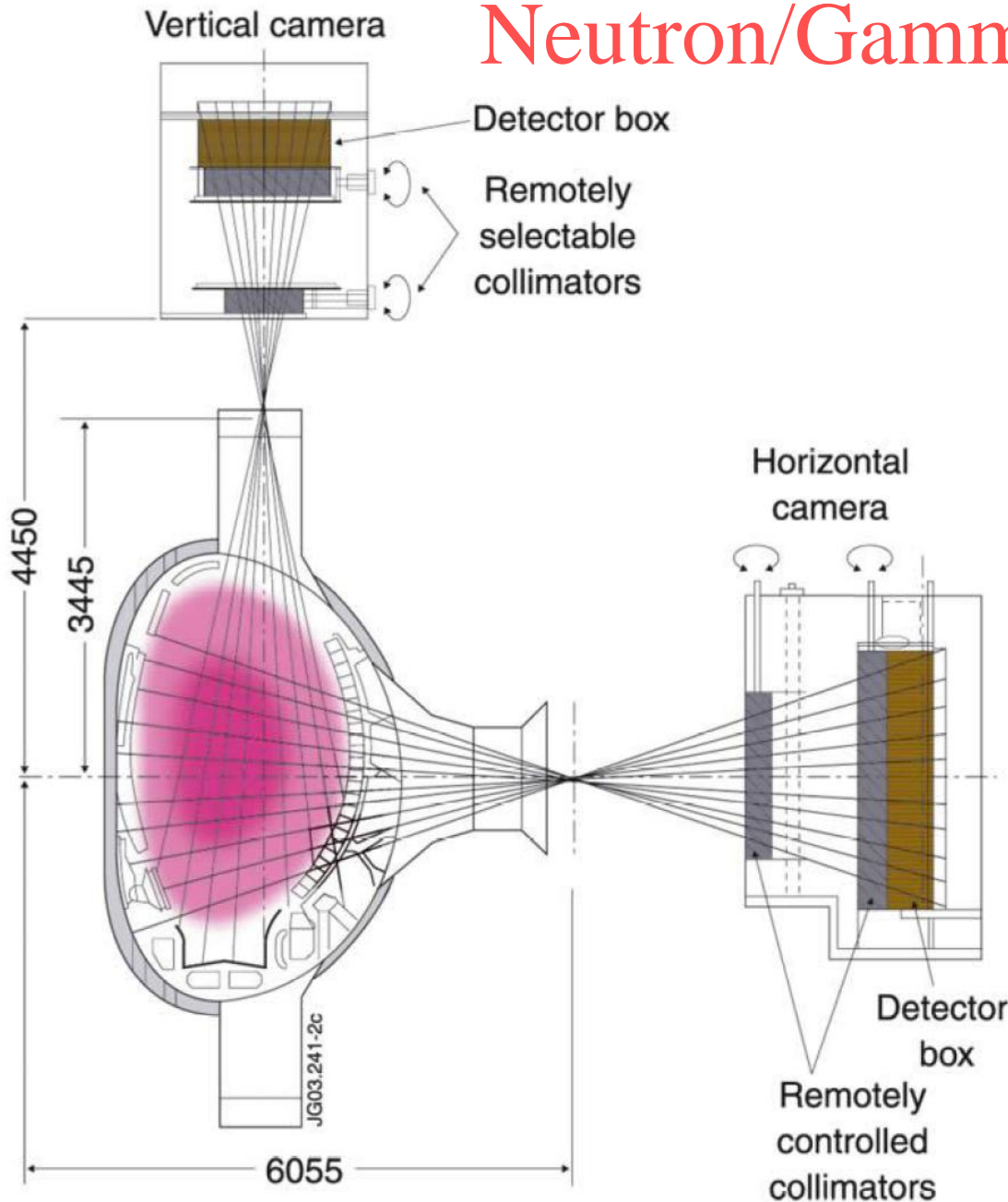
**Bolometry lines of sight:  
300 - 400 channels**

- Bolometry provides time and space resolved 2D profiles of plasma radiation:
  - sensitive from infrared to X-ray region
  - radiation-hard version of the resistive absorbing film bolometer currently in use is under development
  - **access, cooling and radiation hardness** are all issues for bolometer cameras





# Neutron/Gamma Profile Monitor



The neutron and gamma-ray profile monitor represents just one of tens of passive diagnostic methods applied at JET. The monitor has two cameras that allow observations of plasma radiation from ten horizontal and nine vertical directions. In this way we can localize the source of the radiation, in this case the **neutrons produced by fusion or gamma-rays produced by nuclear reactions**. The latter can serve us to trace the presence of fast-ions, in particular helium nuclei (alpha particles).

# Overview of JET Plasma Diagnostics

